

MECHANISMS OF CONTRACTILE DYSFUNCTION
IN THE SENESCENT RAT DIAPHRAGM

By

DAVID S. CRISWELL

A DISSERTATION PRESENTED TO THE GRADUATE SCHOOL
OF THE UNIVERSITY OF FLORIDA IN PARTIAL FULFILLMENT
OF THE REQUIREMENTS FOR THE DEGREE OF
DOCTOR OF PHILOSOPHY

UNIVERSITY OF FLORIDA

1994

ACKNOWLEDGMENTS

I would like to acknowledge those who have been instrumental in this work; particularly my mentor, Dr. Scott Powers and my other committee members: Dr. Stephen Dodd, Dr. Daniel Martin, Dr. Michael Pollock, and Dr. Paul Davenport. They have all given me invaluable guidance and instruction. Further, Drs. Powers and Dodd allowed me to have free run of their laboratories and equipment. These experiments could not have been completed without the technical assistance of my fellow students: Robert Herb, Jeff DeLott, Jane Eason, and Scott Stetson.

I am especially grateful to Dr. Powers for his constant support, example, motivation, and friendship throughout our association.

This work was made possible by funding from the American Lung Association-Florida Affiliate.

TABLE OF CONTENTS

ACKNOWLEDGMENTS	ii
LIST OF TABLES	v
LIST OF FIGURES	vi
ABSTRACT	viii
INTRODUCTION	1
REVIEW OF RELATED LITERATURE	5
Introduction	5
Effects of Aging on Skeletal Muscle	5
Morphological Changes	5
Contractile Changes	6
Biochemical Changes	8
Effects of Aging on the Diaphragm	11
Possible Mechanisms of the Force Deficits in Aging Skeletal Muscle	12
Potential Extrinsic Sources of Age-Related Muscle Dysfunction	12
Potential Intrinsic Mechanisms of Muscle Force-Generating Deficits	14
Summary	17
MATERIALS AND METHODS	18
Animals	18
Experimental Design	18
Experimental Protocol	19
Experimental Procedures	20
Diaphragm Strip <i>in vitro</i> Contractile Measurements	20
Biochemical Measurements	22
Histochemistry	24
Cross-Sectional Area and Specific Force Corrections	27
Diaphragmatic Single Fiber Analysis	28
Statistical Analyses	30
RESULTS	31
Morphometric Characteristics	31
Contractile Properties of the Costal Diaphragm	31
Muscle Composition Measurements	32
Biochemical Measurements	32
Histochemical Measurements	33
Mathematical Correction of Diaphragmatic Specific Force	34
Myofibrillar Protein Correction	34

Muscle Water and Connective Tissue Corrections.	34
Diaphragmatic Single Fiber Specific Force.	35
Myosin Heavy Chain Isoforms and Myofibrillar ATPase Activity.	36
DISCUSSION.....	58
Overview of Principle Findings.	58
Age-Related Changes in Diaphragmatic Force Production.	58
Age-Related Changes in Diaphragm Composition.	59
Diaphragm Cross-Sectional Area and Specific Force Corrections.	62
Diaphragmatic Skinned Single Fiber Measurements.	63
Age-Related Changes in Shortening Velocity of the Diaphragm.	65
Summary and Conclusions.	68
REFERENCES.....	70
BIOGRAPHICAL SKETCH.....	77

LIST OF TABLES

<u>Table</u>	<u>page</u>
1. Morphometric characteristics of adult (9 month old) and senescent (26 month old) F-344 rats	38
2. <i>In vitro</i> contractile properties of costal diaphragm strips from adult (9 month old) and senescent (26 month old) F-344 rats	39
3. Protein composition of costal diaphragm and plantaris from adult (9 month old) and senescent (26 month old) F-344 rats	42
4. Histochemical quantification of connective tissue cross-sectional area in muscle from adult (9 month old) and senescent (26 month old) F-344 rats	44
5. Histochemically determined succinate dehydrogenase (SDH) activity and cross-sectional areas of single fibers from costal diaphragm of adult (9 month old) and senescent (26 month old) F-344 rats	45
6. Costal diaphragm P_0 normalized to muscle cross-sectional area (CSA) and to CSA corrected for non-contractile material in adult (9 month old) and senescent (26 month old) F-344 rats	46
7. Cross-sectional area and calcium-activated force of costal diaphragm skinned single fibers from adult (9 month old) and senescent (26 month old) F-344 rats	50
8. Maximum calcium-activated specific force ($\text{mN} \cdot \text{mm}^{-2}$) of costal diaphragm skinned single fibers classified by MHC phenotype from adult (9 month old) and senescent (26 month old) F-344 rats.....	51
9. Myosin heavy chain (MHC) isoform composition (percent of total MHC pool) of costal diaphragm and plantaris from adult (9 month old) and senescent (26 month old) F-344 rats	55

LIST OF FIGURES

<u>Figure</u>	<u>page</u>
1. Force-velocity relationships for costal diaphragm <i>in vitro</i> strips from adult and senescent F-344 rats.	40
2. <i>In vitro</i> power curves as a function of specific force for combined adult and combined senescent diaphragm strips.	41
3. Photographs of picosirius red/acid fuchsin collagen staining in representative histochemical sections (magnification=400x) from a) adult and b) senescent costal diaphragms.	43
4. Specific isometric force of costal diaphragm <i>in vitro</i> strips expressed both as $N \cdot cm^{-2}$ of muscle cross-sectional area (CSA) and as $N \cdot cm^{-2}$ of myofibrillar CSA. Values are presented for the senescent group (\pm SEM) as a percentage of the adult values. P-value represents statistical comparison of senescent and adult values.	47
5. Specific isometric force of costal diaphragm <i>in vitro</i> strips expressed both as $N \cdot cm^{-2}$ of muscle cross-sectional area (CSA) and as $N \cdot cm^{-2}$ of connective tissue (C.T.)-free CSA, dry CSA, and dry, C.T.-free CSA. Values are presented for the senescent group (\pm SEM) as a percentage of the adult values.	48
6. Correlational analysis of the relationship between costal diaphragmatic specific force and a) relative dry mass of the costal diaphragm (mg/g) and b) relative connective tissue content (mg/g) of the costal diaphragm.	49
7. Specific isometric force of costal diaphragm <i>in vitro</i> strips expressed as $N \cdot cm^{-2}$ of muscle cross-sectional area (CSA) compared to maximum calcium-activated specific force of skinned single fibers expressed as $mN \cdot mm^{-2}$. Values are presented for the senescent group (\pm SEM) as a percentage of the adult values. P-value represents statistical comparison of senescent and adult values.	52
8. Photograph of sodium dodecyl sulfate-polyacrylamide gel electrophoresis of isolated single fibers from the costal diaphragm. Lane 1: Diaphragm fiber bundle expressing all four MHC isoforms. Lane 2: Single fiber expressing type IIdx MHC. Lane 3: Single fiber expressing type I MHC.	53
9. Comparison of costal diaphragmatic myofibrillar ATPase activity from adult and senescent animals. Values are means \pm SEM.	54

10. Photograph of a typical sodium dodecyl sulfate-polyacrylamide gel electrophoresis of bundles of fibers from the costal diaphragm illustrating the region of the gel containing the myosin heavy chains. Lane 1 contains a senescent sample; lane 2 contains an adult sample. 56
11. Correlational analysis of the relationship between costal diaphragmatic V_{\max} and a) myofibrillar ATPase activity of the costal diaphragm ($\text{nmol} \cdot \text{min}^{-1} \cdot \text{mg}^{-1}$) and b) relative type IIb MHC content of the costal diaphragm. 57

Abstract of Dissertation Presented to the Graduate School of the University of Florida
in Partial Fulfillment of the Requirements for the Degree of Doctor of Philosophy

MECHANISMS OF CONTRACTILE DYSFUNCTION
IN THE SENESCENT RAT DIAPHRAGM

By

David S. Criswell

August 1994

Chairman: Scott K. Powers
Major Department: Exercise and Sport Sciences

The purpose of these experiments was to test the hypothesis that age-related alterations in muscle composition cause the known age-related diaphragmatic specific force deficit. Intrinsic properties of the myofibrillar proteins and excitation-contraction (E-C) coupling in the rat costal diaphragm were assessed via an isolated skinned single fiber preparation. Secondly, the hypothesis that the age-related increase in diaphragmatic shortening velocity (V_{max}) is caused by alterations in the senescent diaphragm myosin heavy chain (MHC) phenotype was examined. Isometric twitch and tetanic contractile properties as well as isotonic force-velocity relationships were measured *in vitro* on costal diaphragm strips from adult (9 month old; $n=12$) and senescent (26 month old; $n=13$) specific pathogen free-barrier protected Fischer 344 rats. Costal diaphragm myofibrillar protein concentration, calcium-activated myosin ATPase activity, MHC composition, relative water content, connective tissue (C.T.) concentration, skinned single fiber maximal specific force (specific F_0), succinate dehydrogenase activity, and histochemical relative connective tissue cross-sectional area (CSA) were also measured. Diaphragmatic maximal tetanic force (P_0) normalized to strip CSA was 16.4% lower in the senescent diaphragms

($21.03 \pm 0.4 \text{ N} \cdot \text{cm}^{-2}$) compared to the adult ($25.16 \pm 0.5 \text{ N} \cdot \text{cm}^{-2}$) ($P < 0.001$). There was a trend for myofibrillar protein concentration to be lower (12.5%) in the senescent diaphragms compared to the adult ($P = 0.09$), while diaphragm water content was significantly higher in the senescent group ($P < 0.01$). Histochemical analysis of C.T. CSA revealed a 19.3% increase in the relative contribution of C.T. to the total CSA in the senescent diaphragms ($P = 0.01$). Normalizing diaphragmatic P_0 to dry mass, C.T.-free CSA eliminated the senescent specific force deficit ($P > 0.05$). In agreement, normalizing P_0 to myofibrillar protein CSA resulted in no age group differences in specific force ($P > 0.05$). Specific F_0 of costal diaphragm fibers did not differ between age groups ($P > 0.05$). Diaphragmatic V_{\max} was 17.5% higher in the senescent diaphragms compared to the adult ($P < 0.001$). This change was accompanied by a three-fold increase in the relative proportion of type IIb MHC ($P < 0.001$). Correlational analysis indicated that ~30% of the variance in V_{\max} could be predicted by changes in type IIb MHC composition ($r = 0.56$; $P < 0.05$). These data support the hypothesis that the decline in *in vitro* maximal specific force observed in the senescent costal diaphragm can be explained by age-related alterations in the composition of the diaphragm muscle and the resulting reduction in myofibrillar protein concentration.

INTRODUCTION

The diaphragm is the primary muscle of inspiration and is essential for maintenance of normal ventilation in mammals. It is well established that humans exhibit an age-related decline in maximal inspiratory pressure (1, 2) suggesting that the diaphragm may be subject to aging effects similar to other skeletal muscles. Further, a recently published report (3) as well as data from our laboratory indicate that the senescent rodent displays a reduction (as compared to young animals) in the maximal diaphragmatic force generating capacity normalized to the cross-sectional area of the muscle (i.e. specific force). This age-related diaphragmatic dysfunction may reduce the ability of the aging individual to perform coughing maneuvers and/or to maintain normal ventilation during an acute challenge such as exercise or an asthma attack.

These experiments were designed to define the functional and phenotypic changes associated with aging in the diaphragm of male Fischer 344 rats, and to determine the intrinsic cellular mechanism(s) responsible for the observed age-related decline in the maximal isometric specific force of the diaphragm. Since the age-related diaphragmatic specific tension deficit is observed in an *in vitro* preparation where the muscle is stimulated to contract via an electrical field, the underlying mechanism must be intrinsic to the muscle. In theory, one the following intrinsic mechanisms must be altered by the aging process, thereby, resulting in a decrease in the maximal isometric specific tension of diaphragm muscle: 1) myofibrillar protein concentration (i.e. the number of force-generating units in parallel per unit area); 2) intrinsic properties of the contractile proteins (i.e. the amount of force produced per force-generating unit); 3) excitation-contraction (E-C) coupling (e.g. the

amount of free calcium in the myoplasm during maximal activation); or 4) some combination of these.

The amount of force generated by a muscle is dependent on the number of half-sarcomeres in parallel (4). Therefore, to accommodate differences in the number of parallel cross bridges in parallel due to the size of the muscle, force generation is typically expressed relative to the cross-sectional area of the muscle (specific force). However, this procedure is limited by the assumption that the relative contribution of myofibrillar protein to the total muscle cross-sectional area remains constant. In fact, it has recently been established that hindlimb unweighting and denervation which result in a reduction in specific force also result in a reduction in myofibrillar protein concentration and that this accounts for much of the specific force deficit (5). This suggests the possibility that the observed age-related diaphragmatic specific force deficit may also be explained by a reduction in myofibrillar protein concentration. Alternatively, hypertrophied muscle caused by synergist ablation results in a reduction in specific force without a change in myofibrillar protein concentration (5); therefore, other factors such as E-C coupling and/or intrinsic properties of the contractile proteins can also mediate a specific force deficit under certain conditions.

The potential contribution of altered myofibrillar protein concentration to the age-related specific force changes observed in *in vitro* diaphragm strips from adult (9 mon. old) and senescent (26 mon. old) Fischer 344 rats is examined in the present study. This is accomplished directly by analyzing the myofibrillar protein concentration of samples from adult and senescent diaphragms. A reduction in the myofibrillar protein concentration necessitates an increase in non-contractile volume. Therefore, the present experiments also sought to determine which specific muscle compartment(s) (i.e. myofibrillar protein, connective tissue and/or water) were altered by the aging process. After determining the concentration of each component, the CSA of the separate compartments were calculated by modifying the formula used to calculate average total muscle CSA (see Materials and

Methods). This allows assessment of the relative importance of changes in each of the major muscle components in mediating the age-related diaphragmatic specific force deficit.

The potential contribution of age-related alterations in excitation-contraction coupling to the decline in specific force in the aging diaphragm is assessed by examining the maximum specific force characteristics of individual skinned single fibers isolated from the diaphragms of adult and senescent Fischer 344 rats. Since contraction and relaxation of skinned single fibers is accomplished by directly changing the $[Ca^{++}]$ in the medium bathing the myofibrils, this technique by-passes the excitation-contraction coupling mechanism and therefore provides an assessment of its role in the age-related specific force deficit.

In addition to the specific force deficit observed in the senescent diaphragm, we have also found a significant increase in maximal velocity of shortening (V_{max}) of diaphragm strips from old animals as compared to young adults (unpublished observations). Therefore, the present experiments were also designed to further document this paradoxical change and determine if it is mediated by changes in the relative proportions of the myosin heavy chain (MHC) isoforms and/or biochemically determined myosin ATPase activity.

The following specific hypotheses were tested:

- 1) Diaphragmatic myofibrillar protein concentration is less in senescent (26 mon. old) specific pathogen free-barrier protected (SPF-BP) Fischer 344 rats compared to adult (9 mon. old) SPF-BP Fischer 344 rats.
- 2) The observed deficit in maximal specific force generation in senescent rat diaphragms is explained by the reduction in myofibrillar protein concentration.
- 3) The increase in maximal isotonic shortening velocity in senescent diaphragm strips will be accompanied by, and significantly correlated with an age-related increase in type II MHC expression and myofibrillar ATPase activity.

4) Maximal force generation per CSA in isolated skinned single fibers from senescent rat diaphragms does not differ from the specific force generation of fibers from adult diaphragms.

REVIEW OF RELATED LITERATURE

Introduction

A decline in locomotor skeletal muscle strength and speed of contraction with advancing age has been commonly observed in both humans and animals. Indeed, an overall loss of muscle mass is evident in senescence with the aging effects being most prominent in muscles containing higher proportions of fast-twitch fibers. This age-related atrophy and loss of muscle performance has the potential to severely reduce the functional capacity of an individual.

It is the purpose of this review to discuss the known effects of aging on skeletal muscle with emphasis on the diaphragm. Further, this review will examine several possible mechanisms underlying the age-related muscle dysfunction observed in humans and animals with special attention placed on the force deficits reported in aging skeletal muscle.

Effects of Aging on Locomotor Skeletal Muscle

Morphological Changes

Among the most consistent findings in skeletal muscle with advancing age is a general muscle atrophy (6, 7, 8, 9). Theoretically, this atrophy could be the result of a reduction in fiber number, a decrease in the cross-sectional area (CSA) of some or all fibers in the muscle, or a combination of these. Lexell et al. (8) studied whole vastus lateralis muscles autopsied from formerly healthy men ranging in age from 15 to 83 years who had

suffered sudden accidental death. By sectioning across the middle of the entire muscle, they determined that muscle atrophy begins at early adulthood and progresses throughout life. The atrophy was associated primarily with a loss of fiber number with all histochemically defined fiber types being equally susceptible. There was also a significant age-related reduction in CSA of the type II fibers which contributed to a lesser extent to the overall atrophy. In contrast to this human study, Daw et al. (7) used the nitric acid digestion technique to precisely quantify the fiber numbers in the soleus and extensor digitorum longus (EDL) muscles of young and old rats. These researchers concluded that a loss of fiber number could explain only approximately 25% of the age-related muscle atrophy in the rat. Presumably the remaining 75% of the overall observed atrophy must have been the result of decreases in the CSA of fibers. Compared to a loss of fiber number, there are more studies implicating the reduction in CSA of type II fibers in the age-related muscle atrophy (10, 11); however, this may be due, in part, to the difficulty in making measurements of total fiber number. Collectively, it seems possible that both mechanisms operate to some extent, the importance of which may vary between different species.

Contractile Changes

Of primary importance in the study of aging in skeletal muscle are the changes in muscle contractile properties. Numerous investigators have reported age-related changes in the force generating properties of muscle in both humans (6, 11) and animals (9, 12, 13, 14). In a large cross-sectional study of 33 young and old men, Klitgaard et al. (6) found large age-related changes in both functional and biochemical properties of the elbow flexion and knee extension muscle groups. Functionally, the old subjects exhibited lower values for maximal isometric force, speed of movement, and specific tension (force per cross-sectional area). Similarly, Larsson et al. (11) studied isometric and dynamic strength changes in the quadriceps of 114 male subjects ranging in age from 11 to 70 years. Both

measures of muscular strength did not differ between adult age groups below age 50 years; however, there was a progressive decline in strength after age 50. Further, the loss of strength correlated closely with an observed selective atrophy of type II fibers.

Longitudinal studies of the effects of aging on human skeletal muscle are rare; however, Aniansson et al. (15) reported strength changes in 23 elderly men over a seven year period. After the seven years, isokinetic strength measures in the vastus lateralis muscle were decreased 10-22% while the CSA of type IIa and IIb fibers were reduced 14-25%.

Unfortunately, reports of age-related contractile changes in *in vitro* preparations of rodent locomotor muscles are less conclusive. In keeping with the consistent finding of overall muscle atrophy with aging, total tetanic force generation is reduced in senescent muscles (12, 13, 14). Most studies also demonstrate a prolongation of contraction time (12, 14), time to peak isometric tension (13), and one-half relaxation time (12, 13, 14). Another important measure of contractile function is the tension generated by the muscle per unit of CSA (i.e. specific tension). An age-related reduction in specific tension would indicate that the force reduction in senescent muscles is due to changes in the contractile apparatus itself. Klitgaard et al. (13) examined male Wistar rats of different age groups (9, 24, and 29 months) and reported a decrease in specific tension with aging in the soleus (predominantly slow twitch muscle) and the plantaris (a mixed fiber type muscle). Brooks and Faulkner (14) reported a reduction in specific tension in the EDL of senescent mice; however, no difference in specific tension was found in the soleus between adult and senescent mice. Fitts et al. (12) found no differences in specific tension of the soleus muscle in Long Evans rats of three age groups (9, 18, and 28 months). Finally, in contradiction to the majority of the literature, Eddinger et al. (9) reported an increase in the specific tension of both fiber bundles and isolated skinned fibers from the soleus of senescent Fischer 344 rats. The explanation for these divergent findings is unclear.

Reports of the maximum rate of unloaded shortening (V_{max}) of aging locomotor muscles *in vitro* are also equivocal with most studies showing either a decrease in V_{max}

with aging (12) or no change in V_{\max} (14). Again, the report of Eddinger et al. (9) contradicts the literature by demonstrating an increase in V_{\max} of fiber bundles from the senescent rat soleus.

In spite of the variable results presented above, overall there appears to be a consensus that skeletal muscle becomes slower and weaker with advancing age and that these changes are due, at least in part, to intrinsic changes in the contractile properties of the muscle.

Biochemical Changes

Metabolic enzymes. In an effort to better understand the mechanisms underlying the observed age-related changes in skeletal muscle morphology and function, many investigators have examined the effects of aging at the protein level using analytical biochemistry and more recently molecular biology techniques. The activity of metabolic enzymes was one of the first biochemical measures to be reported with aging. In early studies of human muscle biopsies, no age-related differences in the activities of oxidative enzymes were observed (16, 17). More recently, studies that have controlled for the activity level of the subjects have shown age-related decreases in muscle oxidative enzyme activities (18) and *in vitro* maximal rate of oxygen consumption measured in muscle biopsy samples (19). Animal studies generally indicate that aging of skeletal muscle results in decreases in the activities of key metabolic enzymes of glycolysis, the Krebs's cycle, and β -oxidation (10, 20, 21, 22).

Histochemical fiber types. Another variable reported to change with advancing age is the distribution of ATPase histochemically determined fiber types (23). As mentioned earlier, Lexell et al. (8) concluded that the loss of muscle fibers with age affected all fiber types equally; nevertheless, this issue remains equivocal. Larsson et al. (11) reported an increase in the percent by number of type I fibers in the gastrocnemius of aging humans

while data from Klitgaard et al. (6) failed to show any changes in fiber type distributions in biopsies from senescent human vastus lateralis or biceps brachii. It should be emphasized that most human studies of muscle fibers (e.g. Larsson et al. (11) and Klitgaard et al. (6)) rely on a single needle biopsy and therefore sample only a very small portion of the muscle. Lexell et al. (8), however, studied cross-sections of the entire muscle and, therefore, would seem to provide more reliable data concerning the aging effects on fiber type distribution.

Studies of the aging rat indicate a pattern of fiber type shifts from fast (i.e. type IIa and IIb) to slow (type I). The most consistent finding seems to be an increase in the relative proportion (both by number and by CSA) of type I fibers in predominantly slow-twitch muscles like the soleus (9, 20, 24) and the sartorius (25). Aging affects on fiber types in predominantly fast-twitch muscles are less clear. In the rectus femoris, Kovanen and Suominen (20) reported an age-related decrease in the number of type IIb fibers and a concomitant increase in the number of type IIa fibers. Larsson et al (25) and Eddinger et al. (24) failed to show any age-related change in the fiber type distribution of the EDL. However, in a subsequent report, Eddinger et al. (9) reported an increase in the percentage (both by number and by CSA) of type IIb fibers in the EDL muscles of senescent barrier raised Fischer 344 rats.

Myosin isoform expression. Histochemically determined fiber types are based on the pH stability/lability of the various isoforms of the myosin heavy chains whereon lies the myofibrillar ATPase activity. Employing the techniques of immunohistochemistry and electrophoretic separation of myosin heavy chains (MHC) from individual fibers, it has been established that some proportion of muscle fibers express more than one MHC and/or myosin light chain (MLC) isoform (26, 27). This leads to the conclusion that ATPase histochemistry which classifies fibers into distinct groups and subgroups may overlook subtle changes in the phenotypic expression of fibers in response to aging or any other stimulus. This is evident in the report of Klitgaard et al. (6) in which no age-related change in the distribution of fiber types was observed, but the relative proportion of MHC I was

significantly elevated in comparison to the young group. This overall increase in the percentage of MHC I in the muscle from aging subjects could be due to the selective atrophy of type II fibers as reviewed above; however, in a companion paper by the same authors (27) they report an increase in the incidence of MHC coexpression in the muscle fibers of elderly subjects. This seems to indicate an age-related change at the level of gene expression in favor of MHC I as well as possibly the selective loss of CSA from fibers containing primarily MHC IIa or IIb.

Recent evidence from our laboratory (28) suggests a fiber type specific effect of aging on skeletal muscle with the general aging trend being to reduce the proportion of the faster MHC isoform(s) present in the muscle and to increase the proportion of the slower MHC isoform(s). Specifically, we found a significantly lower percentage of MHC IIb isoform and a concomitantly higher percentage of MHC's IIa, IIdx, and I in the mixed gastrocnemius muscle of 24-month-old specific pathogen free-barrier protected (SPF-BP) Fischer 344 rats compared to 4-month-old rats. Further, the plantaris also showed an age-related decrease in the percentage of MHC IIb and an increase in the percentage of MHC IIdx. Finally, the soleus demonstrated a complete disappearance of the MHC IIa band in the old animals and a concomitant increase in the percentage of MHC I (28). These data are in agreement with recently published reports of increases in the relative proportion of MHC IIdx with concomitant decreases in MHC IIb proportions in aging locomotor muscle from non-barrier protected rats (29, 30).

Myofibrillar ATPase activity. Quantitative myosin ATPase activity is known to correlate closely to the speed of shortening of the intact muscle as well as to the MHC profile of the muscle (4). The evidence indicates agreement between this measure and measures of V_{max} and MHC profile. In other words, ATPase activity decreases with age (31, 32, 33) which corresponds to a shift in MHC from fast to slow and a decrease in V_{max} . It should be noted that work by Florini and Ewton (34) using Fischer 344 rats raised in a specific pathogen-free barrier protected colony has argued that the changes in

biochemical and functional properties observed in aging muscle may be secondary to exposure to some unknown environmental pathogen and therefore, not directly the result of aging. Specifically, Florini and Ewton (34) reported no difference between the myofibrillar ATPase activity of skeletal muscle in young and old barrier protected rats.

Effects of Aging on the Diaphragm

Although limited data exists, the rodent diaphragm may respond to aging in a manner similar to that of other skeletal muscles. Zhang and Kelsen (3) reported a general contractile dysfunction in the diaphragms of aging golden hamsters with reductions in specific tension and V_{\max} and a prolongation of the time to peak tension and one-half relaxation time. Gosselin et al. (35) reported an age-related shift in MHC isoforms from fast to slow in both the crural and costal regions of the rat diaphragm. It should be noted that these authors did not separate the various isoforms of fast MHC (IIa, IIdx, and IIb). In fact, a more recent report from Gosselin et al. (36) indicated a significant increase in the relative proportion of MHC IIb and concomitant decreases in the proportions of MHC IIa and IIdx in the diaphragm of senescent (24 mon. old) SPF-BP Fischer 344 rats compared to 6 mon. old adults. Recent work in our laboratory employing the *in vitro* diaphragm strip preparation has confirmed an age-related increase in diaphragmatic type IIb MHC proportion and has shown significant increases (~25%) in the V_{\max} of 24 mon. old SPF-BP Fischer 344 rats as compared to 4 mon. old rats. However, maximal tetanic isometric specific tension was found to be reduced (~11%) in the 24 mon. old diaphragms (unpublished observations).

This age-related increase in V_{\max} appears to be peculiar to the diaphragm. Since the diaphragm must maintain its work load throughout life, perhaps an age-associated reduction in specific tension could not be met with a reduction in usage of the muscle, as would be possible in locomotor muscles. The MHC shift towards type IIb and the resulting right shift of the force/velocity relationship may serve to increase the power output of the

diaphragm at any given load. The possible mechanism(s) for this suggested adaptation remains to be elucidated.

Interestingly, there appears to be no age-related decline in the activities of metabolic enzymes in the rat diaphragm (35, 37); nor do we find any evidence of fiber atrophy in any fiber type in the senescent rat diaphragm (38, 39). Presumably this is due to the chronic activity of the diaphragm and may indicate that the work of breathing does not change significantly with aging in the rat.

Possible Mechanisms of the Force Deficits in Aging Skeletal Muscle

The remainder of this review will focus on the age-related force deficits reported in locomotor and diaphragm muscle as reviewed above.

Potential Extrinsic Sources of Age-Related Muscle Dysfunction

The observed changes in skeletal muscle occurring with advancing age must have some underlying mechanism(s). These changes may originate within the muscle itself, or they may be secondary to changes occurring in other organ systems which in turn affect the muscle tissue. This section will briefly examine age-related changes in the nervous and endocrine systems and how they may relate to altered muscle function.

Altered neural function. Many of the animal studies reporting a decline in muscle force production with aging have employed maximal direct or field stimulation of the muscles, thereby, eliminating direct effects of the nervous system. For this reason, this review will not deal in depth with age-related changes in the nervous system. Nevertheless, it is well documented that chronic changes in the neural activity patterns of neurons innervating skeletal muscles have profound effects on the phenotype and functional characteristics of the muscle (40). For example, Larsson (41) has suggested that some of

the age-related changes in muscle result from a gradual loss of large alpha-motoneurons which innervate type II fibers and a subsequent reinnervation of some of these fibers with smaller motoneurons. Indeed, this could explain the transition of fiber types and MHC profile from fast to slow that is commonly observed in locomotor muscle with aging as well as the overall loss of fiber number; however, assuming that there are no differences in the intrinsic force generating capabilities of the various MHC isoforms (4, 42), this would not explain the age-related reductions in specific force.

Altered endocrine function. Several hormones have direct or indirect actions on skeletal muscle. One of the most important of these is thyroid hormone which plays an important role in the normal development and differentiation of muscle. Nwoye et al. (43) studied hypo- and hyperthyroidism induced in male rats and reported that thyroid hormone exerted its effects on skeletal muscle even in the absence of normal neural innervation, thereby demonstrating a direct action of thyroid hormone on muscle. Further, Izumo et al. (44) documented changes in the specific mRNA's associated with the various isoforms of MHC with hypo- and hyperthyroidism. These changes were found to be tissue specific with hyperthyroidism resulting in an increase in the mRNA of the MHC isoform associated with the greatest ATPase activity. For example, in the soleus which contains MHC I (~90%) and MHC IIa (~10%), hyperthyroidism resulted in an increase in the mRNA for MHC IIa and a decrease in the mRNA for MHC I. Conversely, in the EDL which contains MHC IIa (~10%) and MHC IIb (~90%), hyperthyroidism resulted in an increase in the mRNA for MHC IIb and a decrease in the mRNA for MHC IIa. Hypothyroidism was found to exert the opposite effects. These findings seem to indicate that thyroid hormone exerts its effects on skeletal muscle by directly altering the phenotype of individual muscle fibers.

With regard to force development, both hyperthyroidism (45) and hypothyroidism (46, 47, 48) have been shown to cause locomotor muscle atrophy and therefore a reduction in the total force production of skeletal muscles as compared to euthyroid controls.

However, when the force is normalized to CSA of the muscle, no differences were found. In contrast to this, data from our laboratory indicates a reduction in the maximal specific tension of diaphragm strips from young adult hypothyroid rats (unpublished observations). Although it has been established that the aging rat exhibits a progressive decline in mean serum thyroid hormone (49, 50), this would not appear to explain the maximal specific tension deficits observed in senescent locomotor muscle. In the diaphragm, however, it appears that an age-related hypothyroidism could contribute to the reduction in specific tension, but would seem to contradict our observed increase in MHC IIb expression.

In addition to thyroid hormone, other hormones and growth factors are known to exert effects on skeletal muscle. Logically, age-related changes in any of these factors could play a role in the aging of muscle. The insulin-like growth factors, specifically IGF-I, have been shown to be closely linked to skeletal muscle growth and differentiation (51). Addition of IGF-I to the culture medium of primary myofibers produced fibers with significantly larger diameters, higher myosin synthesis rates, a longer myosin half-life, more myonuclei per fiber length, and 187% increase in the accumulation of myosin (52). Sonntag et al. (53) have demonstrated that serum IGF-I is reduced in the senescent rat, thereby suggesting a possible relationship between IGF-I (or growth hormone) and aging muscle.

Potential Intrinsic Mechanisms of Muscle Force-Generating Deficits

Experimental models in which a skeletal muscle is removed from an animal and electrically stimulated (*in vitro*) eliminate the acute influences of factors extrinsic to the muscle. Therefore, the age-related force deficit in skeletal muscle studied *in vitro* must be due to changes intrinsic to the muscle itself. It should be noted that any potential intrinsic changes may be the results of chronic age-related changes in extrinsic factors as reviewed in the previous section. The following paragraphs will address several intrinsic

mechanisms which may be responsible for the observed *in vitro* force deficit in senescent skeletal muscle.

Reduction in myofibrillar protein concentration. The force production of a muscle is directly related to the number of contractile units in parallel (4). Therefore, to compare the intrinsic force generating capacity of two muscles, the total force produced is typically expressed relative to the CSA of the muscle (specific tension). However, the CSA of a muscle includes not only the contractile proteins but also fluid and non-contractile material. The extracellular space occupies 8-25% of the CSA of skeletal muscle from young adult rats (54). With this in mind, the comparison of maximal specific tension between two muscles would only be valid if both muscles exhibited similar ratios of contractile/non-contractile tissue.

One possible intrinsic mechanism for the reduction in skeletal muscle specific tension with aging is a reduction in this ratio (i.e. a decrease in the concentration of myofibrillar protein accompanied by increases in the concentration of non-contractile tissue). It is well established that skeletal muscle connective tissue increases in senescence over young adult muscles. Biochemical determination of collagen concentration in the soleus and EDL muscles of 24-25 month old rats indicates large increases in collagen accumulation (55, 56). Further, quantitative histochemical determination of endomysium connective tissue has shown 50-75% increases in the connective tissue content per unit area in senescent rat soleus and EDL muscles (56, 57). This relative increase in connective tissue could explain much of the specific force deficit associated with aging. The relative water content of aging muscle could also change the ratio of contractile/non-contractile material. It has recently been reported that hindlimb unweighting in rats, which is known to cause a reduction in specific force generation of the soleus, also causes an increase in the interstitial fluid volume of this muscle (58). This increase in fluid content along with a reduction in the total content of myofibrillar protein appears to explain the specific force deficit observed in the unweighted soleus muscles (5, 58). Although no age-related alterations in muscle water

content have been reported in locomotor muscles (14), no data are available for the aging diaphragm. Therefore, the relative increase in connective tissue and a potential increase in water content both remain as possible explanations for the diaphragmatic specific force deficit associated with aging.

Finally, the ratio of contractile/non-contractile tissue could also be altered by a reduction in the expression of the myofibrillar proteins. Jaiswal and Kanungo (59) reported that transcription rate and mRNA levels of the skeletal alpha actin gene are reduced in 30 mon. old Wistar rats as compared to 6 mon. old rats. These researchers found no age differences in the transcription rate or mRNA for the MHC genes. Although limited data exists, the studies reviewed here suggest that aging in skeletal muscle is associated with a down-regulation of some of the myofibrillar protein genes accompanied by no change or possibly an up-regulation of some of the non-contractile proteins.

Intrinsic properties of the myofibrillar proteins. Another potential mechanism for the age-related force deficit in muscle is the possibility of intrinsic aging changes in the skeletal muscle proteins. Srivastava and Kanungo (33) reported an age-related decline in the availability of titratable thiol groups in myosin isolated from rat skeletal muscle. Since the thiol groups associated with the MHC molecule are essential for normal myosin ATPase activity, these researchers concluded that age-related changes in the conformational shape of the MHC molecule may explain the decline in myofibrillar ATPase activity and *in vitro* shortening velocity in senescent skeletal muscle (33). If aging does indeed alter the intrinsic properties of the myofibrillar proteins, this could also contribute to the reduction in specific tension independent of changes in the concentration of myofibrillar protein.

Excitation-contraction coupling mechanism. Stimulation of a muscle via a nerve or artificially via electrical current results in muscular contraction by stimulating the sarcoplasmic reticulum (SR) to release free calcium into the myoplasm. This represents a third independent point in the contraction mechanism where aging could affect maximal specific force production. Theoretically, aging could affect multiple sites in the SR and/or

myoplasm that could result in a reduction in the free calcium level during contraction. Recent studies have reported that SR vesicles isolated from the skeletal muscle of old rats exhibit a lower protein content and a reduced maximal calcium storage capacity when compared to vesicles from young rats (60, 61).

Summary

In conclusion, the effects of aging on skeletal muscle may originate extrinsically (e.g. from age-related changes in the neural or endocrine systems) or intrinsically (e.g. aging effects on the muscle genome). In either case, however, the intrinsic properties of the muscle are affected such that maximal force generation per CSA is reduced. This could occur by 1) decreasing the content of myofibrillar protein in the aging muscle, 2) increasing the content of non-contractile tissue in the muscle, 3) altering the structure and therefore the function of the myofibrillar proteins in aging muscle, 4) altering the excitation-contraction coupling mechanism in aging muscle, or 5) a combination of some or all of these factors.

MATERIALS AND METHODS

Animals

Adult (9 mon. old) and senescent (26 mon. old) specific-pathogen-free, barrier-protected (SPF-BP) male Fischer 344 rats were obtained from the National Institute of Aging (NIA). An animal model was chosen because the invasive nature of the proposed experiments precludes the use of human subjects. The Fischer 344 rat is widely accepted and recommended as a standard model of aging (62). Further, the physiological function and fiber type distribution of the rat diaphragm resembles the human diaphragm. SPF-BP rats were chosen, as suggested by Florini and Ewton (34), to ensure that the measured effects were due to aging rather than to undocumented diseases.

Experimental Design

To test the hypotheses listed earlier (Introduction), healthy young adult and senescent rats were examined for diaphragmatic *in vitro* contractile properties, myofibrillar protein content, muscle morphometry, muscle water content, muscle connective tissue concentration, and single skinned fiber maximal specific tension. Twenty-five male SPF-BP Fischer 344 rats were individually housed and fed rat chow and water *ad libitum* while being maintained on a 12/12 hour light/dark photoperiod for ~14 days prior to beginning the experiments. During this 14 day period, animals were handled daily to reduce contact stress. The animals were then assigned to one of two experimental groups based on age.

Group 1) adults (9 months old; n = 12)

Group 2) senescent adults (26 months old; n = 13)

This project was approved by the University of Florida Institutional Animal Care and Use Committee (IACUC) and followed the guidelines for animal use established by the American Physiological Society.

Experimental Protocol

Animals were euthanized by intraperitoneal injection of sodium pentobarbital (90mg/kg) and the entire diaphragm quickly removed and placed in a dissecting dish. A small strip of the costal diaphragm (~0.3 x ~2.0 cm) was carefully cut leaving a portion of the central tendon and the rib attachment on the ends. This strip was utilized for *in vitro* measurements of contractile function; specifically, peak isometric twitch tension, one-half relaxation time, maximal rate of twitch tension development, peak isometric tetanic tension, and isotonic force-velocity relationship. All contractile measurements were conducted with the muscle at L_0 .

The remaining diaphragm was carefully trimmed of fat and connective tissue (including the central tendon), blotted and weighed on a Mettler analytical balance. The costal portion of the diaphragm was then divided into five pieces: piece #1 was frozen in liquid nitrogen and stored at -70°C for subsequent measurement of myofibrillar protein concentration, Ca^{++} -activated myosin ATPase activity, and myosin heavy chain profile; piece #2 was weighed and frozen in liquid nitrogen for subsequent measurement of muscle water content; piece #3 was frozen in liquid nitrogen for subsequent measurement of connective tissue concentration; piece #4 was placed on aluminum foil at resting excised length and frozen in liquid nitrogen, for subsequent histochemical sectioning (ATPase fiber typing, quantitative histochemical succinate dehydrogenase activity, and connective tissue); piece #5 was stored in relaxing solution at 5°C for subsequent single fiber measurements.

In order to provide a locomotor muscle comparison to the effects of aging on the diaphragm, the right and left plantaris muscles were also removed, weighed, frozen in

liquid nitrogen and stored at -70°C for measurement of myofibrillar protein concentration, myosin heavy chain profile, Ca^{++} -activated myosin ATPase activity, muscle water, and connective tissue content.

Experimental Procedures

Diaphragm Strip *in vitro* Contractile Measurements

Muscle preparation. After reaching a surgical plane of anesthesia, the entire diaphragm was removed and placed in a dissecting chamber containing a Krebs-Henseleit solution equilibrated with a 95% O_2 / 5% CO_2 gas. A muscle strip was dissected out from the ventral costal region and suspended vertically between two light weight plexiglas clamps in a jacketed tissue bath containing Krebs-Henseleit and $12\mu\text{M}$ d-tubocurarine to produce complete neuromuscular blockade. One clamp was fixed while the other was connected to a transducer (Cambridge Technology, model 300B). The Cambridge transducer is a combined force and position transducer and is capable of monitoring both isometric and isotonic contractions. The force on the lever can be electronically controlled from 0 to 80 g while the length change of the muscle is monitored, or the length of the muscle can be held constant while force is monitored. The jacketed tissue bath was aerated with gas (95% O_2 / 5% CO_2), pH was maintained at 7.4, and the osmolality of the bath was ~ 290 mOsmol. Temperature in the organ bath was maintained at $\sim 24 \pm 0.5^{\circ}\text{C}$ since higher temperatures result in a deterioration of muscle function (63). After 15 min equilibration in the bath, the muscle strip was field stimulated along its entire length with platinum wire electrodes using a modified Grass Instruments S48 stimulator. A supramaximal stimulation voltage was used equal to $\sim 150\%$ of the minimum voltage necessary for maximal activation of the muscle (~ 140 volts). We have demonstrated in pilot

experiments that this method of stimulation results in maximal force generation when compared to direct muscle stimulation using stainless steel electrodes.

After the 15 minute equilibration period, the muscle strip was adjusted to its optimum contractile length (L_0) at which maximal tetanic tension is obtained; this was accomplished by systematically adjusting the length of the muscle using a micrometer while evoking tetanic contractions (140 volts, 330 msec train duration, 50 Hz, and 2 msec pulse width). After finding L_0 , a series of isometric twitch contractions (~6-8, separated by 2 min rest intervals), a series of isometric tetanic contractions (~4-6, separated by 3 min rest intervals), and a series of isotonic tetanic contractions (12-15, separated by 2 min rest intervals) were performed in random order. Following completion of the protocol, L_0 was measured using calipers with the strip still suspended between the two plexiglas clamps.

Isometric twitch contractions. Peak isometric twitch tension was determined from a series of single pulses (140 volts, 2 msec duration). The Cambridge transducer output was amplified and differentiated by operational amplifiers and underwent A/D conversion for analysis using a computer based data acquisition system (GW Instruments-Series II). In addition, half relaxation time (i.e. the time required for force to fall from maximum to half-maximum; $(1/2 RT)$), and maximal rate of tension development were determined by computer analysis of the force transduced output.

Peak isometric tetanic tension. A series of isometric tetanic contractions was produced using a supramaximal (140 V) stimulus train of 50 Hz, 2 msec pulse width, and 1000 msec duration (modified Grass Instruments S48 stimulator). Force was monitored by the computerized ergometer previously described. Each tetanic contraction was separated by a three minute recovery period.

Force-velocity measurements. The relationship between force and muscle shortening velocity was assessed by measurement of shortening velocity (Cambridge transducer model 300B) at ~12 isotonic loads (100 msec trains of 2 msec pulses at 50Hz) over the range of ~2-90% of maximal isometric tension (P_0). The force-velocity data was fit to the Hill

equation (64) using least-squares techniques, and maximal velocity of unloaded shortening (V_{\max}) was determined by solving for velocity when force equals zero.

Biochemical Measurements

Myofibrillar protein concentration. Myofibrillar protein was isolated using a modification of the myofibril extraction technique described by Solaro et al. (65); myofibrillar protein concentration was then determined using the biuret technique of Watters (66). Briefly, the diaphragm and plantaris portions designated for myofibrillar protein analysis were thawed and placed in a petri dish on ice. The muscle was then carefully cleaned of fat and tendon and scissor minced. Precisely 100 mg of muscle was then homogenized using a glass on glass homogenizer in 4 ml of sucrose buffer (250 mM sucrose, 100 mM KCl, 5 mM EDTA, 20 mM Tris, pH = 6.8) and centrifuged for 15 min. at 2500 x g. The supernatant was discarded and the pellet suspended in a KCl buffer containing Triton X-100 to eliminate membrane ATPase components (175 mM KCl, 0.5% Triton X-100, 20 mM Tris, pH = 6.8). This was centrifuged for 10 min at 2500 x g and the supernatant discarded. The pellet was again suspended in the KCl buffer containing Triton X-100 and centrifuged at 2500 x g. This process was repeated in a KCl buffer (175 mM KCl, 20 mM Tris, pH = 7.0) yielding a myofibrillar protein pellet of sufficient purity for quantitative assessment of myofibrillar concentration (46).

This technique does not separate the insoluble connective tissue proteins from the myofibrillar proteins. Since connective tissue concentration changes with aging, this would not represent a constant error. Therefore, a more accurate myofibrillar protein concentration was obtained by subtracting the connective tissue concentration (mg/g) as determined by the method of Segal et al. (67) from the myofibrillar protein concentration (including connective tissue) (mg/g) as determined by the method described above. The coefficient of variation for this technique is ~7% in our laboratory.

Calcium-activated myosin ATPase activity. Immediately after measurement of myofibrillar protein concentration, myosin ATPase activity was determined on the samples using the technique described by Caiozzo et al. (46). Briefly, myofibrillar protein is incubated in the presence of a maximally activating level of Ca^{++} ($\text{pCa} = 4.0$), and ATP. The myosin ATPase enzyme hydrolyzes ATP to form ADP + Pi. Following cessation of the reaction by addition of trichloroacetic acid, the concentration of Pi is determined via the Fiske-Subbarow reaction (Sigma Chemical, St. Louis, MO).

Myosin heavy chain composition. The remaining myofibrillar protein (after biuret and ATPase assays) was used for separation of myosin heavy chain (MHC) isoforms using sodium dodecyl sulfate (SDS)-polyacrylamide gel electrophoresis. The myofibrillar protein was diluted in glycerol to a concentration of ~ 1 mg/ml (the samples can be stored in this form at -20°C for up to two months). These glycerol samples were further diluted to a concentration of ~ 0.25 mg/ml in sample buffer containing 62.5 mM Tris ($\text{pH}=6.8$), 1.0% SDS, 0.01% bromophenol blue, 15.0% glycerol, and 5.0% β -mercaptoethanol. The protein was then denatured by incubation at $\sim 95^\circ\text{C}$ for 3 min.

One to three μg of protein was loaded onto 22 cm vertical gels (Biorad Protean IIXi) composed of 8% acrylamide and 40% glycerol. The samples were electrophoresed for 20 hours at $\sim 5^\circ\text{C}$ using a constant voltage required to attain an initial current of 12 milliamps per gel (68). Following electrophoresis, the gels were stained with Coomassie Blue R-250 for 30 min and destained in 30% methanol, 7% acetic acid for two hours. The relative proportions of the myosin isoform bands (percent of total myosin pool) were analyzed using a computer-based image analysis system (Targa M8 image capture board, Truevision; Java video analysis software, Jandel Scientific) integrated with a high resolution video camera (Video World, Inc.). The region of the gel containing the MHC bands was digitized for each lane and the area and intensity of staining determined in duplicate for each band. In our laboratory, the coefficient of variation for repeated measurement of relative MHC composition of a given sample is $< 3\%$.

Total muscle water content. Determination of total water content in a portion of the costal diaphragm was made using a freeze drying technique incorporating a vacuum pump with a negative pressure of ~ 1mmHg. The frozen samples were placed in the vacuum chamber and dried for 24 hours before measuring the dry mass. The dry mass of the samples was unchanged after an additional 24 hours in the vacuum chamber, thereby confirming complete drying. Relative muscle water content was calculated from the difference between the wet weight of the diaphragm section (taken when the diaphragm was removed from the animal) and the dry weight of the same section.

Connective tissue concentration. Muscle samples were analyzed for total protein concentration and connective tissue concentration using the techniques described by Segal et al. (67). Briefly, muscle sections were homogenized in 0.9% NaCl and allowed to stand 18 hours in 0.05 M NaOH to solubilize nonconnective tissue. Total muscle protein concentration was measured from a sample of the intact digest. The remaining NaOH digest was centrifuged for 15 min at 4000 x g to sediment collagenous protein. The protein concentration of the supernatant was measured and the connective tissue protein concentration calculated as the difference between protein concentration of the intact digest and that of the digest supernatant. This technique has been shown to be a sensitive measure of muscle connective tissue (54, 69).

Histochemistry

Succinate dehydrogenase. A portion of the costal diaphragm was blotted dry and carefully placed flat on a square of aluminum foil. The muscle was then frozen by dipping the foil directly into liquid nitrogen. Care was taken to insure that all samples were frozen at the same unstressed excised length to avoid length-mediated variations in fiber cross-sectional area. Frozen sections (10 μm thickness) of the diaphragms were cut using a cryostat (Reichert-Jung) at - 20° C. The activity of succinate dehydrogenase (SDH) was

quantitatively determined in individual fibers of the diaphragm cross-sections using the technique of Blanco et al. (70) and analyzed using a light microscope (Nikon-Alphaphot) interfaced with a computerized image analysis system. Briefly the rationale and techniques for this procedure are as follows. Since SDH is a mitochondrial membrane-bound enzyme, it will not diffuse out of histochemically prepared cross-sections. This makes SDH a good candidate for quantitative histochemical analysis. The principle of the Blanco et al. (70) assay involves the progressive reduction of nitroblue tetrazolium (NBT) by electrons released from the oxidation of succinate (the SDH reaction) to form a colored compound (NBT-dfz) which serves as a reaction indicator.

To measure muscle fiber SDH activity, two to three cryosections were placed on a cover slip and stored at -20°C until assay. Within 5 min. of removal from the -20°C environment, the muscle sections were introduced into a Columbia jar containing the reaction medium (5 mM EDTA, 0.75 mM sodium azide, 1.0 mM methoxyphenazine methosulphate, 1.5 mM nitroblue tetrazolium, 80 mM succinate, 100 mM phosphate buffer, pH=7.6). The reaction was stopped at exactly 3 min. by multiple rinses in distilled water. The cover slips were then mounted and the sections digitized using a computerized image analysis system (described earlier under "Myosin Heavy Chain Composition") interfaced with a light microscope. The rate at which the reaction indicator was deposited within a fiber (i.e. SDH activity) is calculated using the Beer-Lambert equation:

$$[\text{NBT-dfz}] / \text{min.} = \Delta \text{O.D.} / k \times L$$

Where $\Delta \text{O.D.}$ = the optical density change per minute measured at 570 nm (optical density is defined as $\log [1/\% \text{ transmission}]$), k = the molar extinction coefficient for NBT-dfz (26,478 O.D. units / mole \cdot cm), and L = the length of the light path through the tissue (10 μm thickness). The system was calibrated for optical density measurements and cross-sectional area before and after analysis of each tissue section using neutral density filters and a stage micrometer, respectively. Approximately 100 fibers from each muscle section were analyzed. After an image of the muscle section is digitized, a cursor controller is used

to outline individual cells. The O.D. of the cell is determined by the average O.D. of all pixels contained within the outlined cell. The Δ O.D. is determined by subtracting the O.D. of the tissue section incubated without substrate from the measured O.D. of each cell and dividing by the three minute reaction time. A photograph of a serial section stained for myofibrillar ATPase was used to identify the fiber type of each cell analyzed for SDH activity. We have previously reported this technique to be valid and reliable as compared to a biochemical assay of SDH activity in muscle homogenate (71). Approximately 100 fibers (30-40 of each fiber type) were sampled from each of ten adult and ten senescent costal diaphragms.

ATPase fiber typing. Serial sections of the same diaphragms were used for histochemical ATPase fiber typing (23) based on the acid lability/stability of the various MHC ATPase isoforms. The relative proportions of the fiber types (I, IIa, and IIb) and their cross-sectional areas were determined using computerized planimetry calibrated with a stage micrometer.

Connective tissue histochemistry. The technique of Constantine (72) was used to stain serial sections for connective tissue. This procedure combines Picro Sirius Red and Acid Fuchsin to selectively stain both large and small collagen fibers. Further, this technique has been used to report age-related quantitative changes in connective tissue content of locomotor muscle cross-sections (57). Briefly, this dye stains connective tissue bright red while leaving other tissues unstained. When the sections are visualized through a green filter (570 nm) the connective tissue appears black and the remaining tissue white. The stained sections were dehydrated, mounted with permount, and analyzed using the computer based image analysis system by which the video signal of the section was converted to a graphic image with two levels of gray (i.e. black and white). Computerized planimetry was then used to quantitatively assess the number of black pixels (i.e. stained for connective tissue) within a given calibrated area. In order to calculate the relative proportion of the total CSA taken up by connective tissue for each sample, the entire

diaphragm section was analyzed (5-7 digitized images) excluding damaged or folded regions if any.

Cross-Sectional Area and Specific Force Corrections

After the length of the muscle strip (L_o) and its mass were carefully determined, the muscle strip cross-sectional area (CSA) was calculated using the formula:

$$\text{CSA (cm}^2\text{)} = \text{muscle mass (g)} / [\text{muscle length (cm)} \times \text{muscle density (g/cm}^3\text{)}]$$

Assuming muscle density = 1.056 g/cm³ (73).

Myofibrillar protein CSA was calculated for the diaphragm strips using the same formula with the exception that myofibrillar content (g) (i.e. myofibrillar protein concentration (g/g) x strip mass (g)) was substituted for strip mass. This calculation assumes that purified myofibrils have the same density as whole muscle. Although this may not be the case, the difference would be small and should produce only a small and constant effect on the CSA values obtained for both experimental groups. Likewise, connective tissue CSA and dry mass CSA were also calculated using this formula substituting strip connective tissue content (g) and dry mass content (g) for total strip mass, respectively.

The maximal isometric force generated by each of the diaphragm strips was then normalized to muscle CSA (specific force (P_o)), myofibrillar CSA, connective tissue-free CSA (strip CSA - connective tissue CSA), dry mass CSA, and dry mass, connective tissue-free CSA (dry mass CSA - connective tissue CSA).

The dry mass, connective tissue-free CSA of the strips was also determined independently by an alternate method employing the histochemical connective tissue staining procedure. The contribution of connective tissue to the total dehydrated CSA of the histochemical sections (i.e. cm² of connective tissue / cm² dehydrated CSA) was determined as described above. The connective tissue CSA (cm²) of each strip was then

calculated by multiplying this relative connective tissue CSA (cm^2/cm^2) by the dry mass CSA (cm^2). Maximal tetanic force was then normalized to the histochemically determined dry mass, connective-free CSA (dry mass CSA - histochemical connective tissue CSA).

The total CSA of the costal diaphragm was calculated for each animal from the total costal mass and the measured L_0 of the *in vitro* strips. The total potential force production (N) of each costal diaphragm was then estimated by multiplying the specific P_0 ($\text{N} \cdot \text{cm}^{-2}$) by the total CSA (cm^2). (Note: This procedure assumes that all fibers in the costal diaphragm have the same L_0 . This introduces some error into the calculation. However, if the geometry of the costal diaphragm does not differ between adult and senescent animals, this would be a small, constant error.)

Diaphragmatic Single Fiber Analysis

Fiber preparation. A bundle of muscle fibers cut from the costal region of the diaphragm was stored in a relaxing solution containing 7.0 mM EGTA, 1.0 mM free Mg^{++} , 4.38 mM ATP, 14.5 mM creatine phosphate, 20 mM imidazole, and sufficient KCl to adjust ionic strength to 180 mM. This solution chemically removes the sarcolemma from the fibers; fiber bundles can be stored up to 30 days in this solution (74). Activating solutions of varying calcium concentrations were made by addition of CaCl_2 to relaxing solution in the appropriate amounts to yield free calcium concentrations of $\text{pCa}=4.0$ and $\text{pCa}=3.0$ (75).

Single fiber mechanical measurements. Five to ten single fibers were dissected from each diaphragm sample for measurement of calcium-activated maximal isometric force production. Individual fibers were attached on one end to a fixed clamp and on the other to a sensitive isometric force transducer (Cambridge Technology model 400A) and suspended horizontally above a plexiglas block containing multiple wells ($\sim 400\mu\text{l}/\text{well}$). A solution containing no calcium (relaxing solution) and a solution containing a maximally activating

concentration of calcium ($pCa = 4.0$ to $pCa = 3.0$) were pipetted into the separate wells producing a meniscus which protrudes above the top surface of the plexiglas block. The block was then manually moved such that the fiber was positioned within the meniscus of the desired solution. At this point, the length of the fiber was set by employing an eyepiece micrometer to adjust the fiber to 120% of its resting length (resting length was defined as the point where the slack has just been removed). In approximately 50% of the fibers, the sarcomere length was also determined by directing the beam of a helium-neon laser (Spectra-Physics) to the fiber and observing the primary diffraction pattern. The distance between the primary diffraction lines is inversely proportional to the sarcomere length and was calibrated by first directing the laser through a grid of known dimensions on a microscope slide. Sarcomere length was set at $2.5 \mu m$ and maintained at this length during the force measurements. The force developed during maximal calcium activated contractions did not differ in the same fiber between the two methods of setting fiber length. Fiber diameter was measured at multiple sites along the length of the fiber with a calibrated microscope eyepiece micrometer. Fiber diameter was used to calculate fiber cross-sectional area, assuming the fiber is a cylinder.

Movement of the fiber from well-to-well followed the sequence: relaxing solution, calcium solution, relaxing solution; this sequence was repeated four to six times (separated by 2 min rest intervals) with the fiber being exposed to activating solutions of $pCa = 4.0$ and $pCa = 3.0$, to insure maximal activation. The force developed did not differ between the two calcium concentrations. If the same force could not be achieved ($\pm 5\%$) at least three times, the fiber was discarded. Force generation by the fiber was measured and monitored by the force transducer interfaced to a computer and utilizing the same data acquisition system described above for diaphragm strip measurements.

Myosin heavy chain characterization. Following the contractile measurements, the fibers were dissolved in $10 \mu l$ of sample buffer and incubated at $95^\circ C$ for 3 minutes to

denature the proteins. The entire volume (10 μ l) was then electrophoresed as described previously for characterization of MHC profile (68).

Statistical Analyses

Comparisons between experimental groups (adult vs. senescent adult) for each dependent variable with the exceptions of histochemical SDH data, isolated skinned single fiber data, and MHC isoform distribution data were made by unpaired Student t-tests. Histochemical single fiber SDH activities and CSA were analyzed by a 2 x 3 (age x fiber type) factorial analysis of variance (ANOVA). Isolated skinned single fiber F_0 , CSA, and specific F_0 were analyzed by unpaired t-tests for type I and type II fibers with the Bonferroni procedure applied to correct for multiple comparisons. Myosin heavy chain isoform distribution was analyzed by a 2 x 4 (age x MHC phenotype) factorial ANOVA with special contrasts applied to determine where differences occurred. The relationships between biochemical measures (e.g. myofibrillar protein concentration) and contractile properties (e.g. maximal tetanic specific tension) were determined by Pearson product moment correlation. Significance was established at $P < 0.05$.

RESULTS

Morphometric Characteristics

Mean (\pm SEM) body mass and morphometric characteristics of the diaphragm and plantaris muscles for both experimental groups are presented in table 1. Body mass did not differ between groups. Likewise, costal diaphragm mass did not differ between groups, therefore the ratio of costal diaphragm mass to total body mass did not differ between groups. Further, the dimensions of the costal diaphragm *in vitro* strips (length and CSA) taken at L_0 were not different between groups. There was however, a strong trend for crural diaphragm mass to be higher in the senescent animals as compared to the adults ($P=0.06$). Conversely, plantaris muscle mass tended to be lower in the senescent group as compared to the adult ($P=0.07$), causing a tendency for the plantaris mass / body mass ratio to be reduced in the senescent animals ($P=0.06$).

Contractile Properties of the Costal Diaphragm

Table 2 reports the *in vitro* contractile properties (means \pm SEM) of costal diaphragm strips taken from adult and senescent animals. Maximal tetanic force expressed per cm^2 of strip CSA was 16.4% lower in the senescent diaphragms as compared to the adults. Assuming a constant fiber length at L_0 , the total CSA of each diaphragm was calculated based on each costal diaphragm mass and the measured L_0 of the *in vitro* strip. Using this total costal CSA (cm^2) and the measured specific force ($\text{N} \cdot \text{cm}^{-2}$), the potential for total maximal tetanic force generation (N) for each costal diaphragm was estimated. Since

diaphragmatic mass and strip L_0 did not differ between groups and the specific force was reduced in the senescent group, the estimated total potential force generation by the costal diaphragm was significantly lower in the senescent animals compared to the adults.

In vitro twitch characteristics (1/2 relaxation time and rate of tension development) did not differ between the two experimental groups. Analysis of the isotonic force-velocity relationship fitted with the Hill equation (64) indicated a 17.5% increase in V_{max} of the senescent diaphragm strips as compared to the adult strips ($P < 0.001$). The a/P_0 ratio differed statistically between adult and senescent groups ($P = 0.02$) indicating greater curvature in the force-velocity relationship of the senescent diaphragm strips compared to the adult strips. The Hill equation was fitted to the force-velocity data from each *in vitro* strip individually to calculate V_{max} and the a/P_0 ratio. However, for illustrative purposes, figure 1 presents the Hill equation fitted to the combined data for each age group. Finally, maximal power of the diaphragm strips, calculated from the isotonic force-velocity data, did not differ between age groups. Figure 2 displays the combined data illustrating the relationship between diaphragmatic power and specific force for each age group.

Muscle Composition Measurements

Biochemical Measurements

Myofibrillar protein concentration, connective tissue protein concentration, and dry mass per unit wet mass results (means \pm SEM) are presented in table 3 for the costal diaphragm and plantaris muscles of adult and senescent rats. Costal diaphragm myofibrillar protein concentration tended to be lower ($P = 0.09$) in the senescent group and connective tissue concentration tended to be higher ($P = 0.06$) compared to the adult group. Further, relative dry mass content (mg dry mass/g wet mass) was significantly lower in the senescent diaphragms compared to the adults. The total diaphragmatic contents of

myofibrillar protein, connective tissue, and water were calculated by multiplying the appropriate concentration by the total costal weight for each animal. Mean (\pm SEM) values (adult vs. senescent) were as follows: total myofibrillar protein: 75.1 \pm 4.2 vs. 70.2 \pm 3.3 mg ($P=0.37$), total connective tissue: 20.2 \pm 3.4 vs. 29.6 \pm 3.1 mg ($P=0.05$), and total water: 534 \pm 26 vs. 589 \pm 14 mg ($P=0.07$).

For the plantaris muscle, myofibrillar protein concentration tended to be lower in the senescent muscles compared to the adult ($P=0.11$). Further, connective tissue protein concentration was significantly higher in the senescent muscles when compared to the adult plantaris muscles ($P=0.02$). Finally, plantaris dry mass concentration did not differ between groups.

Histochemical Measurements

Histochemical determination of connective tissue cross-sectional area. Table 4 presents the relative contribution of connective tissue to the total cross-sectional area of dehydrated histochemical sections of the costal diaphragm and plantaris muscles from adult and senescent rats. Figure 3 illustrates representative cross-sections of adult and senescent costal diaphragms stained for collagen. The relative proportion of connective tissue CSA to total CSA was 19.3% higher ($P=0.01$) in the senescent diaphragms and 51.1% higher ($P<0.001$) in the senescent plantaris muscles compared to the adult diaphragms and plantaris muscles, respectively.

Succinate dehydrogenase activity. Histochemically determined succinate dehydrogenase (SDH) activity and cross-sectional areas of costal diaphragm single fibers classified by fiber type are presented in table 5. The CSA of the type I, type IIa, and type IIb fibers in the senescent costal diaphragms did not differ from the CSA of fibers with the corresponding phenotype in adult costal diaphragms. Also, the SDH activity of individual costal diaphragm fibers did not differ between groups in any of the three fiber types.

Likewise, the average SDH activity for the entire costal diaphragm cross-section did not differ between age groups (adult mean(\pm SEM) = 4.82 ± 0.12 vs. senescent mean(\pm SEM) = 4.67 ± 0.11 mmol \cdot min $^{-1}$ \cdot liter $^{-1}$). In contrast, the average SDH activity for the plantaris muscle was significantly lower ($P=0.02$) for the senescent group compared to the adult (adult mean(\pm SEM) = 2.03 ± 0.15 vs. senescent mean(\pm SEM) = 1.41 ± 0.18 mmol \cdot min $^{-1}$ \cdot liter $^{-1}$).

Mathematical Correction of Diaphragmatic Specific Force

Table 6 presents the maximum tetanic force (P_o) produced by the *in vitro* diaphragm strips normalized to muscle CSA, connective tissue (C.T.)-free CSA, dry mass CSA, and dry mass, C.T.-free CSA.

Myofibrillar Protein Cross-Sectional Area Correction

Mean (\pm SEM) cross-sectional areas of the *in vitro* diaphragm strips did not differ between the experimental groups (adult = 0.0215 ± 0.001 cm 2 vs. senescent = 0.0201 ± 0.001 cm 2). However, myofibrillar protein CSA was significantly lower ($P=0.003$) in the senescent diaphragm strips (0.00181 ± 0.00006 cm 2) compared to the adult strips (0.00215 ± 0.00009 cm 2). When P_o for each diaphragm strip was normalized to its myofibrillar protein CSA, the resulting specific force did not differ between age groups (table 6, figure 4).

Muscle Water and Connective Tissue Corrections

Mean (\pm SEM) C.T.-free CSA was not different between groups (adult = 0.0208 ± 0.001 cm 2 vs. senescent = 0.0193 ± 0.001 cm 2), while calculation of dry mass

CSA of the strips resulted in significantly lower values ($P=0.03$) for the senescent group ($0.00485\pm 0.0003\text{ cm}^2$) compared to the adult ($0.00598\pm 0.0004\text{ cm}^2$). Calculation of dry mass, C.T.-free CSA using the biochemical measurement of C.T. concentration resulted in even greater differences ($P=0.007$) between adult and senescent values (adult = $0.00536\pm 0.0003\text{ cm}^2$ vs. senescent = $0.00407\pm 0.0003\text{ cm}^2$). Also, calculation of dry mass, C.T.-free CSA using the histochemical measurement of C.T. CSA (adult = $0.00525\pm 0.0003\text{ cm}^2$ vs. senescent = $0.00435\pm 0.0002\text{ cm}^2$) was in close agreement with the biochemical method.

The age-related deficit in mean specific force observed when P_0 was normalized to muscle CSA (-16.4%) was lower when P_0 was normalized to C.T.-free CSA (-15.5%). However, this was not significantly different. When P_0 was normalized to dry mass CSA, the senescent mean specific force deficit was significantly reduced (-6.4%). Finally, normalization of P_0 to dry mass, C.T.-free CSA of the strip completely eliminated the senescent specific force deficit (table 6, figure 5).

Figure 6 illustrates the relationships between dry mass of the costal diaphragm and specific force ($P=0.005$) and between connective tissue concentration and specific force ($P=0.03$). The coefficients of determination for the relationships between dry mass and connective tissue concentration and specific force are $r^2=0.31$ and $r^2=0.18$, respectively.

Diaphragmatic Single Fiber Specific Force

Table 7 presents mean (\pm SEM) cross-sectional areas, maximal calcium-activated force (F_0), and maximal specific force of isolated diaphragmatic skinned single fibers. Because of the low sample size, all fibers exhibiting type II MHC phenotype (type IIa, type IIx, and type IIb) were analyzed together. Specific forces of individual fibers classified by MHC phenotype for each animal are presented in table 8. In type I fibers, CSA, F_0 , and specific F_0 did not differ between adult and senescent groups. In type II fibers, there were

trends for both CSA and F_0 to be lower in the senescent fibers compared to the adult fibers; however, specific F_0 did not differ between groups. Figure 7 compares the specific force of senescent type I and type II skinned single fibers to the specific force of senescent *in vitro* diaphragm strips (both expressed as a percentage of the corresponding adult mean value). The age-related specific force deficit present in the diaphragm strips is not present in the calcium-activated single fiber preparation (figure 7). Figure 8 illustrates the identification of MHC phenotype of single diaphragmatic fibers using polyacrylamide gel electrophoresis (PAGE).

Myosin Heavy Chain Isoforms and Myofibrillar ATPase Activity

Figure 9 illustrates mean (\pm SEM) calcium-activated myofibrillar ATPase activity for the adult and senescent costal diaphragms. Senescent diaphragms tended to exhibit higher ATPase activities as compared to the adults, however, this was not significant ($P=0.20$).

The relative myosin heavy chain isoform composition (mean \pm SEM) of the costal diaphragm and plantaris is presented in table 9. Paradoxically, the relative proportions of both the type I MHC ($P<0.001$) and the type IIb MHC ($P<0.001$) were found to be higher in the senescent diaphragms compared to the adult. Concomitantly, the proportion of type II_{dx} MHC was significantly lower ($P<0.001$) in the senescent diaphragms when contrasted to the adults. In the plantaris, there was a trend for the percentage of type IIb MHC to be lower ($P=0.12$) in the senescent muscles, while the proportion of type I MHC was significantly higher ($P<0.001$) in the senescent plantaris compared to the adult muscles. Figure 10 shows a PAGE separation of the MHC isoforms illustrating the notable relative increase in the type IIb MHC band in a senescent diaphragm sample as compared to a typical adult diaphragm sample.

Finally, figure 11 illustrates the relationships between myofibrillar ATPase activity of the costal diaphragm and V_{max} ($P=0.07$) and between percent type IIb MHC in the costal

diaphragm and V_{\max} ($P=0.005$). The coefficients of determination for the relationships between myofibrillar ATPase activity and percent type IIb MHC and V_{\max} are $r^2=0.14$ and $r^2=0.29$, respectively.

Table 1. Morphometric characteristics of adult (9 month old) and senescent (26 month old) F-344 rats.

	Adult (n=12)	Senescent (n=13)	P-value
Body mass (g)	389.3 ± 8.6	392.2 ± 9.1	NS
Costal Diaphragm mass (mg)	738 ± 29	778 ± 19	NS
Crural Diaphragm mass (mg)	334 ± 18	376 ± 12	NS (P=0.06)
Total Diaphragm mass (mg)	1072 ± 46	1154 ± 27	NS (P=0.13)
Costal mass/body mass ratio (mg/g)	1.89 ± 0.06	1.98 ± 0.04	NS
Costal <i>in vitro</i> strip length at L ₀ (mm)	24.8 ± 0.4	24.6 ± 0.4	NS
Right Plantaris mass (mg)	298 ± 15	270 ± 5	NS (P=0.07)
Plantaris mass/body mass (mg/g)	0.77 ± 0.04	0.69 ± 0.02	NS (P=0.06)

Values are means ± SEM.
NS = non-significant (P>0.05).

Table 2. *In vitro* contractile properties of costal diaphragm strips from adult (9 month old) and senescent (26 month old) F-344 rats.

	Adult (n=12)	Senescent (n=13)	P-value
Maximal tetanic P_o ($N \cdot cm^{-2}$)	25.16 \pm 0.46	21.03 \pm 0.38	P<0.001
Total potential force (N)*	7.09 \pm 0.3	6.29 \pm 0.2	P=0.03
1/2 RT (msec)	39.03 \pm 1.1	40.31 \pm 1.8	NS
+dP/dt ($N \cdot msec^{-1} \cdot cm^{-2}$)	0.23 \pm 0.01	0.20 \pm 0.01	NS
V_{max} (lengths $\cdot sec^{-1}$)	5.50 \pm 0.11	6.46 \pm 0.15	P<0.001
a/P_o	0.25 \pm 0.01	0.20 \pm 0.02	P=0.02
Maximal power (mWatts $\cdot cm^{-2}$)	254.61 \pm 9.43	236.50 \pm 10.41	NS

Values are means \pm SEM.

NS = non-significant ($P>0.05$).

P_o = Isometric specific force.

* Total force calculated from total costal diaphragm mass.

1/2 RT = Relaxation half-time following a twitch contraction.

+dP/dt = Maximal rate of specific force development during a twitch contraction.

V_{max} = Maximal shortening velocity calculated from the Hill equation.

a/P_o = Curvature of the force-velocity relationship, where a = a constant derived from the Hill equation.

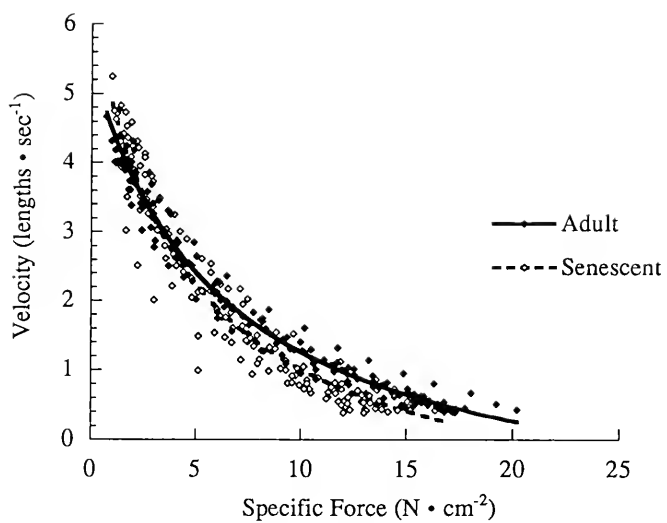


Figure 1. Force-velocity relationships for costal diaphragm *in vitro* strips from adult and senescent F-344 rats.

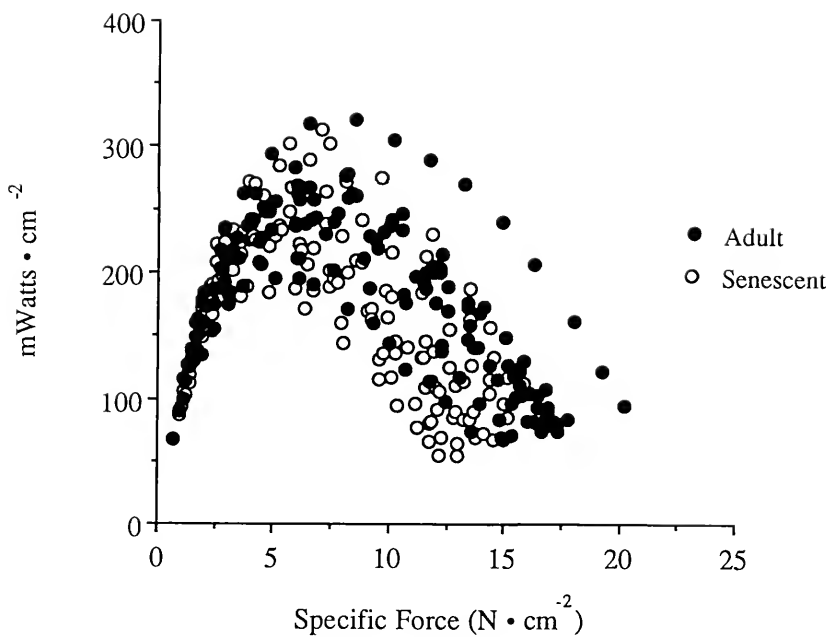


Figure 2. *In vitro* power curves as a function of specific force for combined adult and combined senescent diaphragm strips.

Table 3. Protein composition of costal diaphragm and plantaris from adult (9 month old) and senescent (26 month old) F-344 rats.

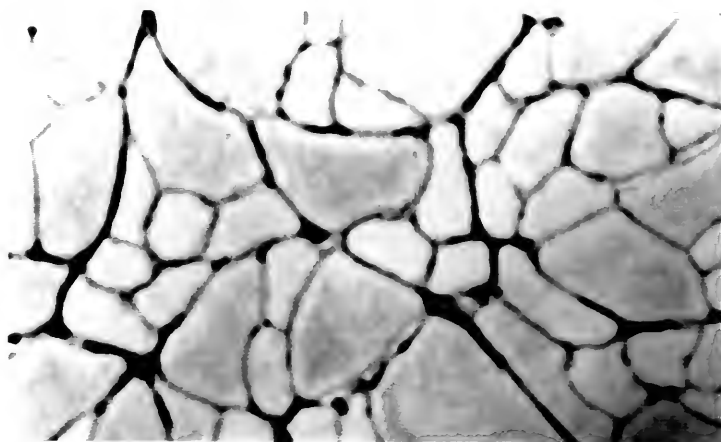
	Adult (n=12)	Senescent (n=13)	P-value
<u>Costal Diaphragm</u>			
Dry mass (mg/g wet mass)	278.5 ± 9.6	240.1 ± 10.2	P=0.003
Myofibrillar protein *	102.9 ± 5.8	90.0 ± 4.5	NS (P=0.09)
Connective Tissue protein (mg/g wet mass)	27.3 ± 4.2	37.9 ± 3.7	NS (P=0.06)
<u>Plantaris</u>			
Dry mass (mg/g wet mass)	256.8 ± 8.2	259.7 ± 3.3	NS
Myofibrillar protein *	106.6 ± 6.1	89.1 ± 7.3	NS (P=0.11)
Connective Tissue protein (mg/g wet mass)	45.6 ± 3.7	66.3 ± 4.4	P=0.02

Values are means ± SEM.

NS = non-significant (P>0.05).

* Does not include connective tissue protein (see Materials and Methods).

A.



B.



Figure 3. Photographs of picrosirius red/acid fuchsin collagen staining in representative histochemical sections (magnification=400x) from a) adult and b) senescent costal diaphragms.

Table 4. Histochemical quantification of connective tissue cross-sectional area in muscle from adult (9 month old) and senescent (26 month old) F-344 rats.

	Adult (n=12)	Senescent (n=12)	P-value
Costal Diaphragm	12.13 ± 0.58	14.47 ± 0.63	P=0.01
Plantaris	11.05 ± 0.38	16.70 ± 1.04	P<0.001

Units are mm² connective tissue per 100 mm² of tissue.
Values are means ± SEM.

Table 5. Histochemically determined succinate dehydrogenase (SDH) activity and cross-sectional areas of single fibers from costal diaphragm of adult (9 month old) and senescent (26 month old) F-344 rats.

	Adult (n=10)	Senescent (n=10)	P-value
<u>Type I fibers</u>			
SDH activity	6.07 ± 0.60	5.91 ± 0.40	NS
CSA (μm^2)	1349 ± 163	1359 ± 72	NS
<u>Type IIa fibers</u>			
SDH activity	6.16 ± 0.59	5.62 ± 0.52	NS
CSA (μm^2)	1424 ± 159	1330 ± 48	NS
<u>Type IIb fibers</u>			
SDH activity	2.36 ± 0.33	2.24 ± 0.32	NS
CSA (μm^2)	3461 ± 202	3290 ± 186	NS

Units of SDH activity are $\text{mmol} \cdot \text{min}^{-1} \cdot \text{liter}^{-1}$ of tissue.

Values are means ± SEM.

NS = non-significant ($P > 0.05$).

Table 6. Costal diaphragm P_0 normalized to muscle cross-sectional area (CSA) and to CSA corrected for non-contractile material in adult (9 month old) and senescent (26 month old) F-344 rats.

	<u>Specific Force ($N \cdot cm^{-2}$)</u>		Δ (%)
	Adult (n=12)	Senescent (n=13)	
Normalized to muscle CSA	25.16 \pm 0.46	21.03 \pm 0.38 ^a	- 16.44
Normalized to C.T. free CSA	25.88 \pm 0.49	21.86 \pm 0.35 ^a	- 15.53
Normalized to dry CSA	91.37 \pm 3.05	85.52 \pm 1.99 ^b	- 6.40
Normalized to dry, C.T. free CSA [*]	101.98 \pm 4.22	100.64 \pm 2.64	NS
Normalized to dry, C.T. free CSA [§]	104.02 \pm 3.53	100.06 \pm 2.48	NS
Normalized to myofibrillar CSA	254.13 \pm 16.13	241.26 \pm 12.08	NS

Values are means \pm SEM.

C.T. = connective tissue

^{*} Biochemical determination of C.T. mass.

[§] Histochemical determination of C.T. CSA.

^a $P < 0.001$

^b $P = 0.12$

NS = non-significant ($P > 0.05$).

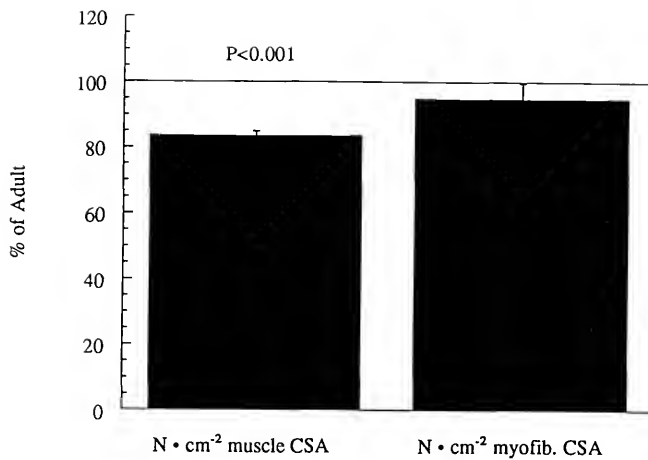


Figure 4. Specific isometric force of costal diaphragm *in vitro* strips expressed both as N • cm⁻² of muscle cross-sectional area (CSA) and as N • cm⁻² of myofibrillar CSA. Values are presented for the senescent group (\pm SEM) as a percentage of the adult values. P-value represents statistical comparison of senescent and adult values.

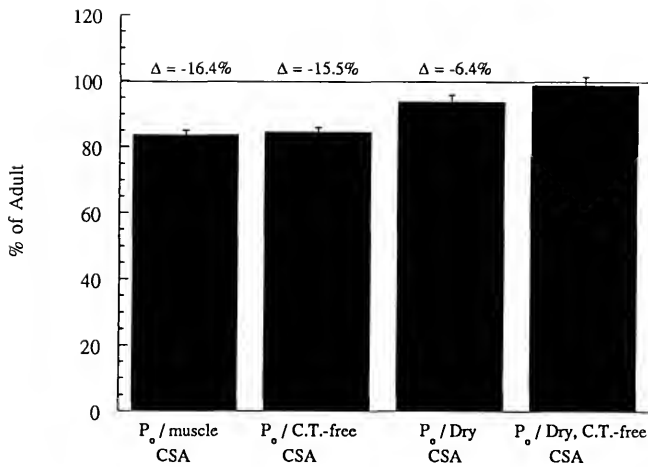
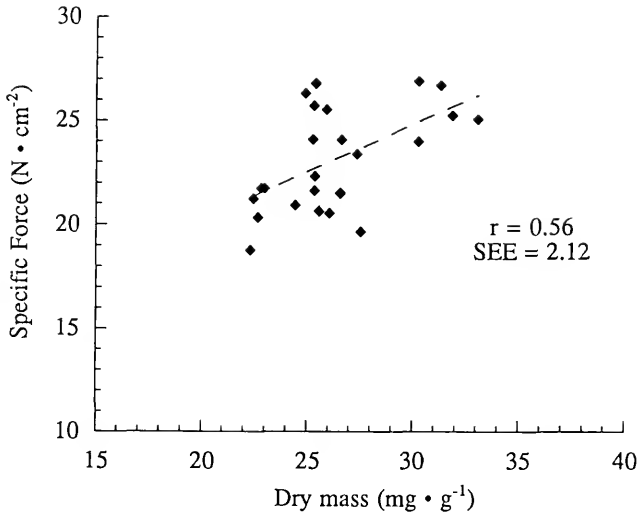


Figure 5. Specific isometric force of costal diaphragm *in vitro* strips expressed both as $N \cdot \text{cm}^{-2}$ of muscle cross-sectional area (CSA) and as $N \cdot \text{cm}^{-2}$ of connective tissue (C.T.)-free CSA, dry CSA, and dry, C.T.-free CSA. Values are presented for the senescent group (\pm SEM) as a percentage of the adult values.

A.



B.

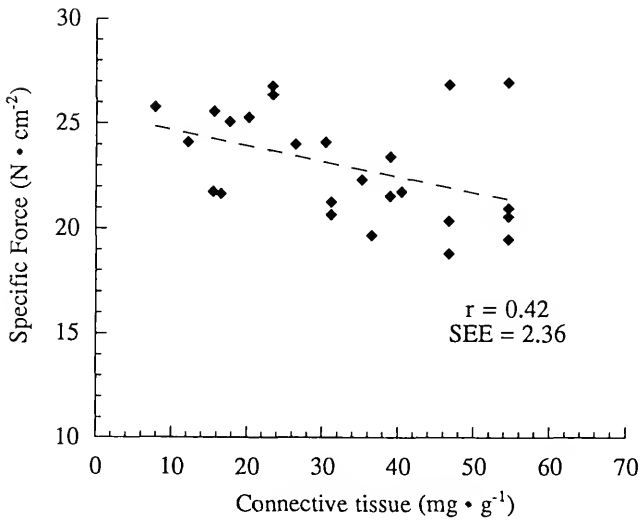


Figure 6. Correlational analysis of the relationship between costal diaphragmatic specific force and a) relative dry mass of the costal diaphragm (mg/g) and b) relative connective tissue content (mg/g) of the costal diaphragm.

Table 7. Cross-sectional area and calcium-activated force in costal diaphragm skinned single fibers from adult (9 month old) and senescent (26 month old) F-344 rats.

	Adult	Senescent	P-value
<u>Type I MHC</u>	<u>n = 19</u>	<u>n = 12</u>	
CSA (μm^2)	1200 \pm 110	1311 \pm 133	NS
F ₀ (mN)	0.073 \pm 0.007	0.077 \pm 0.009	NS
Specific F ₀ (mN \cdot mm ⁻²)	62.5 \pm 6.7	60.9 \pm 6.4	NS
<u>Type II MHC</u>	<u>n = 14</u>	<u>n = 9</u>	
CSA (μm^2)	2481 \pm 273	1750 \pm 235	NS (P=0.08)
F ₀ (mN)	0.182 \pm 0.034	0.107 \pm 0.016	NS (P=0.11)
Specific F ₀ (mN \cdot mm ⁻²)	70.0 \pm 9.3	65.5 \pm 9.3	NS

Values are means \pm SEM.

n = the number of individual fibers across all animals.

F₀ = single fiber maximal calcium-activated tetanic force.

NS = non-significant (P>0.05).

Table 8. Maximum calcium-activated specific force ($\text{mN} \cdot \text{mm}^{-2}$) of costal diaphragm skinned single fibers classified by MHC phenotype from adult (9 month old) and senescent (26 month old) F-344 rats.

	<u>MHC Phenotype</u>			
	Type I	Type IIa	Type IIx	Type IIb
<u>Adult</u>				
Animal #1	76.07 (3)	41.37 (1)	144.73 (1)	94.43 (1)
Animal #2	80.85 (3)			109.04 (1)
Animal #3	69.44 (4)		67.56 (1)	
Animal #4	51.88 (5)			136.22 (1)
Animal #5	50.16 (1)	36.32 (1)	85.85 (1)	
Animal #6	43.21 (3)	55.26 (1)	50.20 (1)	
Animal #7			63.16 (1)	
Animal #8			46.28 (2)	56.25 (1)
Mean \pm SEM:	61.9 \pm 6.3	44.3 \pm 5.7	76.3 \pm 13.3	99.0 \pm 16.7
<u>Senescent</u>				
Animal #1	62.53 (3)			
Animal #2	57.77 (2)			
Animal #3	59.14 (1)			
Animal #4	67.29 (2)			76.64 (2)
Animal #5	39.91 (1)			88.46 (2)
Animal #6	35.91 (1)		88.96 (1)	
Animal #7	97.02 (2)	40.79 (1)	42.30 (2)	
Animal #8			44.69 (1)	
Mean \pm SEM:	57.4 \pm 5.7		58.7 \pm 13.4	82.6 \pm 12.4

The values for each animal represent the mean of (n) fibers expressing that MHC phenotype sampled from the costal diaphragm.

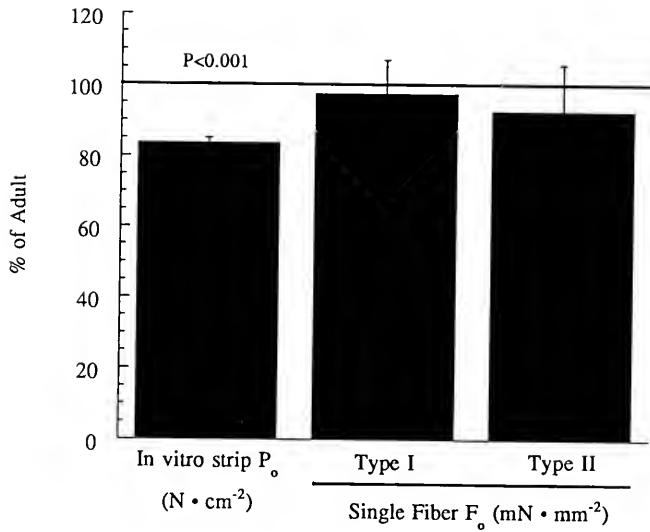


Figure 7. Specific isometric force of costal diaphragm *in vitro* strips expressed as $N \cdot cm^{-2}$ of muscle cross-sectional area (CSA) compared to maximum calcium-activated specific force of skinned single fibers expressed as $mN \cdot mm^{-2}$. Values are presented for the senescent group (\pm SEM) as a percentage of the adult values. P-value represents statistical comparison of senescent and adult values.

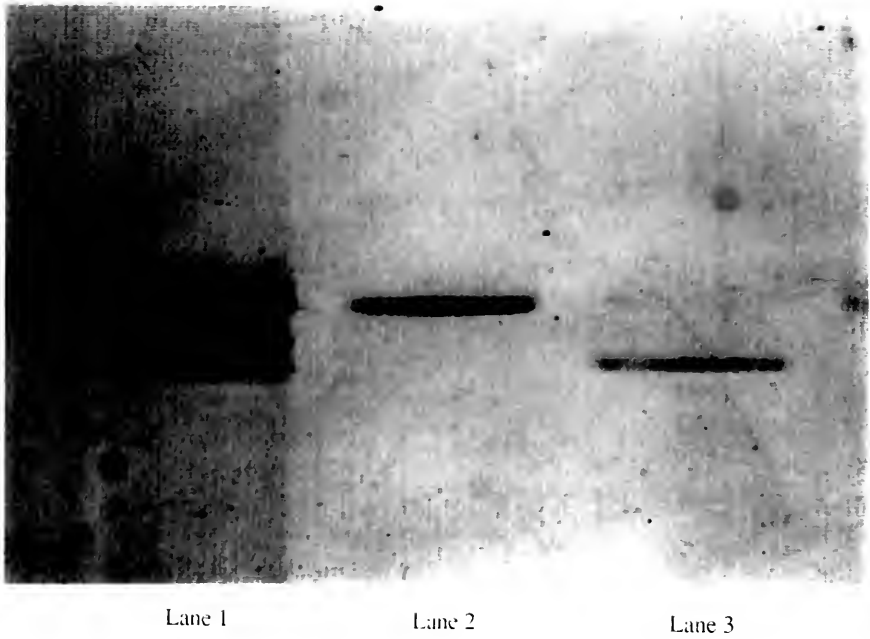


Figure 8. Photograph of sodium dodecyl sulfate-polyacrylamide gel electrophoresis of isolated single fibers from the costal diaphragm.
Lane 1: Diaphragm fiber bundle expressing all four MHC isoforms.
Lane 2: Single fiber expressing type IIcx MHC.
Lane 3: Single fiber expressing type I MHC.

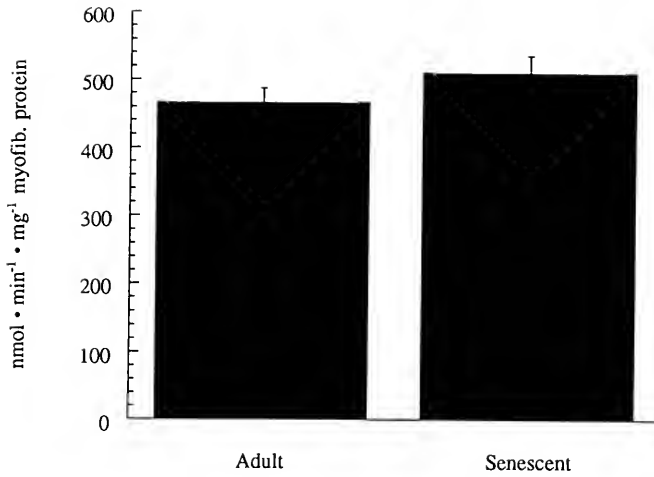


Figure 9. Comparison of costal diaphragmatic myofibrillar ATPase activity from adult and senescent animals. Values are means \pm SEM.

Table 9. Myosin heavy chain (MHC) isoform composition (percent of total MHC pool) of costal diaphragm and plantaris from adult (9 month old) and senescent (26 month old) F-344 rats.

	Adult (n=12)	Senescent (n=13)	P-value
<u>Costal Diaphragm</u>			
Type I MHC	20.4 ± 0.5	24.7 ± 0.7	P<0.001
Type IIa MHC	18.4 ± 1.0	18.2 ± 0.9	NS
Type IIx MHC	54.9 ± 1.3	38.3 ± 1.6	P<0.001
Type IIb MHC	6.3 ± 1.1	18.8 ± 1.3	P<0.001
<u>Plantaris</u>			
Type I MHC	1.5 ± 0.2	3.8 ± 0.5	P<0.001
Type IIa MHC	12.3 ± 0.8	11.2 ± 0.6	NS
Type IIx MHC	64.0 ± 2.5	67.3 ± 1.5	NS
Type IIb MHC	22.2 ± 2.4	17.7 ± 1.4	NS (P=0.12)

Values are means ± SEM.
NS = non-significant (P>0.05).

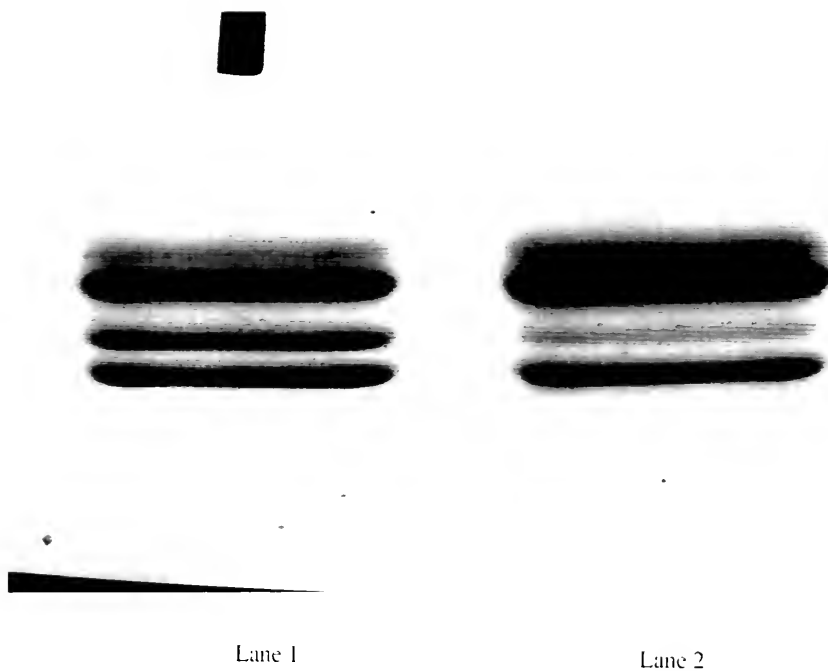
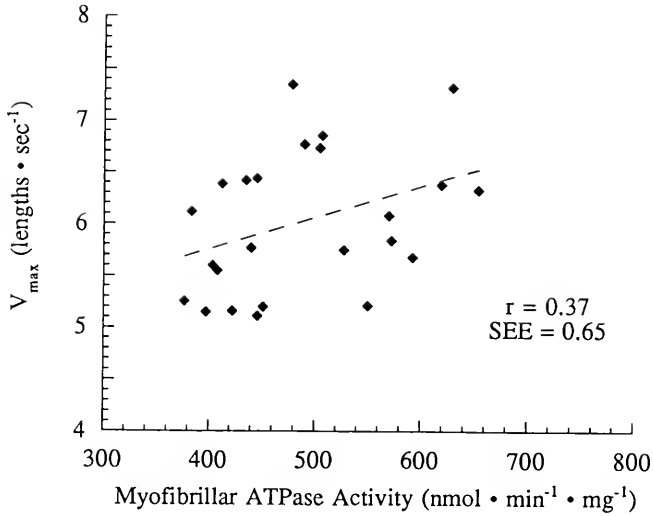


Figure 10. Photograph of a typical sodium dodecyl sulfate-polyacrylamide gel electrophoresis of bundles of fibers from the costal diaphragm illustrating the region of the gel containing the myosin heavy chains. Lane 1 contains a senescent sample; lane 2 contains an adult sample.

A.



B.

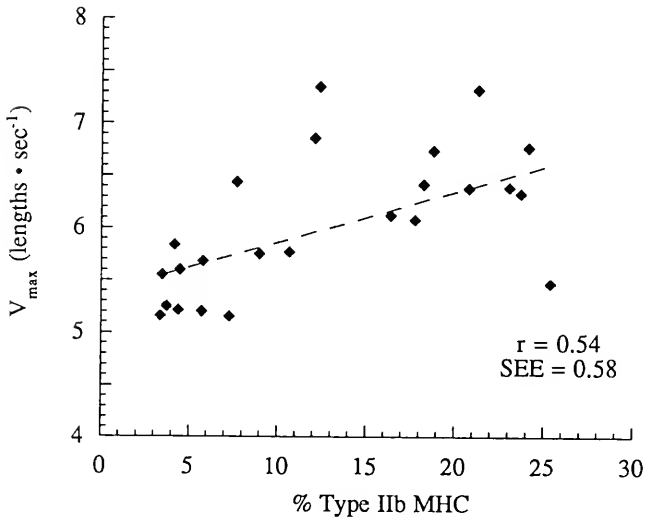


Figure 11. Correlational analysis of the relationship between costal diaphragmatic V_{max} and a) myofibrillar ATPase activity of the costal diaphragm (nmol · min⁻¹ · mg⁻¹) and b) relative type IIb MHC content of the costal diaphragm.

DISCUSSION

Overview of Principle Findings

These experiments confirm the existence of a significant age-related reduction in maximal *in vitro* tetanic specific force (P_o) of the costal diaphragm. The data support the hypothesis (#1) that the composition of the costal diaphragm is altered as the animal reaches senescence with connective tissue and water content increasing and myofibrillar protein concentration tending to decrease. Further, in support of hypothesis #2, it appears that these increased concentrations of non-contractile material in the senescent diaphragm fully account for the observed deficit in specific P_o . This conclusion is corroborated by data that fails to indicate any age-related deficit in calcium-activated maximal specific force of isolated diaphragmatic skinned single fibers (supporting hypothesis #4). Finally, hypothesis #3 is supported by data showing a large increase in senescent diaphragmatic V_{max} compared to adults which is accompanied by a dramatic increase in the relative proportion of type IIb MHC in the costal diaphragm. However, these changes in type IIb MHC proportion do not fully explain the age-related difference in V_{max} . Paradoxically, the percentage of type I MHC was also significantly increased in the senescent diaphragms.

Age-Related Changes in Diaphragmatic Force Production

Several recent studies have reported a reduction in diaphragmatic *in vitro* maximal specific force of aging rodents (3, 36). This is confirmed in the present study wherein specific P_o was found to be 16.4% lower in senescent diaphragms compared to adults. The

body mass of the senescent animals in the present study did not differ from the adult rats; therefore, the effects of growth and maturation on the diaphragm were avoided. One possible mechanism for the senescent specific P_0 deficit is an increase in non-contractile mass (and CSA) with no change in contractile mass. This would effectively reduce the contractile protein concentration by dilution and, therefore, result in a specific P_0 reduction. If this were the case, the total (absolute) force generating capacity of the diaphragm would not be compromised. However, this is not true in the present study. The total mass of the costal diaphragm and the costal mass / body mass ratio did not differ between groups; therefore, the estimated total diaphragmatic force was significantly lower in the senescent animals (table 2). This suggests that the observed specific P_0 deficit in the diaphragm of senescent rats compared to adults translates into a real reduction in the functional capability of the diaphragm to generate inspiratory pressure.

Although no data is available concerning the workload on the senescent diaphragms, activity of the oxidative enzyme, SDH, was unchanged in the senescent diaphragms as compared to the adults whereas SDH activity in the plantaris was ~31% lower in the senescent animals. This is interpreted as evidence that the workload on the diaphragm is similar between senescent and adults animals. Therefore, the age-related reduction in maximal force generating capacity of the diaphragm would reduce the reserve diaphragmatic force available to the senescent animals, which may be needed to maintain adequate ventilation during times such as heavy exercise or periods of airway obstruction. The physiological significance of this age-related reduction in diaphragmatic force generation is unclear.

Age-Related Changes in Diaphragm Composition

If individual cross-bridges produce the same amount of force when activated, the force produced by a muscle is a function of the number of parallel cross-bridges (4). This

forms the basis for the hypothesis that the aging process results in alterations in the composition of the costal diaphragm such that the number of cross-bridges per unit area is reduced (i.e. reduced myofibrillar protein concentration). The major components of skeletal muscle include water, myofibrillar protein, and connective tissue. Conditions other than aging which cause a reduction in skeletal muscle maximal specific P_o , such as hindlimb unweighting and denervation, have recently been shown to be associated with reductions in the concentration of myofibrillar protein (5). On the other hand, compensatory hypertrophy, which also causes a reduction in specific P_o , is not associated with a reduction in myofibrillar protein concentration (5). The present study reveals a strong trend for myofibrillar protein concentration to be lower (-13%) in the senescent diaphragms compared to the adult, but this did not reach statistical significance ($P=0.09$). Mean total myofibrillar protein content (myofibrillar protein concentration (mg/g) x costal mass (g)) was ~8% lower in the senescent diaphragms as compared to the adults, but this also was not statistically significant. The technique used in the present study to assess myofibrillar protein concentration is a modification of a procedure that has been widely used to document changes in locomotor muscle myofibrillar protein concentration following hindlimb unweighting and denervation (5). However, the magnitude of the changes in myofibrillar protein concentration and specific force generation are much greater under these conditions compared to the changes presently observed in the aging costal diaphragm (5, 76, 77). In our hands, the coefficient of variation for this technique is ~7%; hence, this technique may lack the resolution necessary to statistically identify relatively small age-related changes in diaphragmatic myofibrillar protein concentration. Nevertheless, the failure to demonstrate any age-related change in total costal diaphragm mass in the presence of the observed increases in diaphragmatic connective tissue concentration and water content, strongly suggest that myofibrillar protein concentration is reduced in the senescent diaphragms.

It is well established that connective tissue concentration increases with aging in locomotor muscle (78) and diaphragm (79); this is confirmed in the present study. Also, total diaphragmatic connective tissue content (mg) was significantly higher in the senescent diaphragms as compared to the adult.

This is the first study to examine age-related changes in water content of the diaphragm. The aging process reportedly does not alter the water content of locomotor muscles in the rodent (14). This was confirmed in the plantaris muscle of senescent and adult rats in the present study; however, the relative concentration and the total content of water were found to be increased in the senescent diaphragms. The location of the increased diaphragmatic water content (i.e. intracellular vs. extracellular) remains unknown. A recent report has shown that hindlimb unweighting results in an increase in locomotor muscle water content and that this occurs in the interstitial space (58). Therefore, it is possible that aging could result in a similar increase in interstitial water content of the diaphragm muscle. In fact, the observed age-related increase in the water content of the diaphragm may be linked to the accumulation of connective tissue also observed in the senescent diaphragms. One functional property of collagen fibers is that they resist changes in tissue configuration and volume (80). Also, collagen fibers immobilize the glycosaminoglycans (GAG) found in the interstitial space (80). Due to the highly hydrophilic nature of GAGs, these molecules are important in establishing the osmotic pressure of the extracellular space. Therefore, the quantity and type of GAGs present in a tissue greatly influence the interstitial volume of the tissue (80). Given this relationship between collagen content, GAGs, and tissue water content, it seems reasonable to speculate that the increase in connective tissue in the aging diaphragm may result in the accumulation of GAG molecules in the interstitial space of the muscle, thereby, increasing the osmotic pressure and causing an age-related accumulation of water. Future experiments would be necessary to determine the role, if any, that GAGs play in mediating the age-related increase in water content in the costal diaphragm.

In summary, these observations suggest that two mechanisms interact to result in alterations in the composition of the senescent diaphragm. First, an accumulation of water in the diaphragm and second, an accumulation of connective tissue. Although the measured values for myofibrillar protein concentration (mg/g) and content (mg) were not statistically different between the senescent and adult diaphragms, the estimated total diaphragmatic force generation potential, as discussed previously, suggests that total myofibrillar protein content may, in fact, be reduced in the senescent diaphragms.

Diaphragm Cross-Sectional Area and Specific Force Corrections

Kandarian and coworkers (5, 58) have pointed out that the information gained from examining alterations in specific P_0 of muscles is limited by the failure of this procedure to distinguish between intrinsic changes in the contractile machinery and changes in the concentration (or CSA) of the contractile proteins. Taylor and Kandarian (5) have recently introduced a method of normalizing force production of a muscle to the myofibrillar protein CSA rather than to total CSA. This procedure is effective in determining the force generated per unit area of contractile protein. In the present data, the significant mean specific P_0 deficit noted in the senescent diaphragm strips was eliminated when normalized to myofibrillar protein CSA (figure 4). This implies that the age-related reduction in diaphragmatic myofibrillar protein concentration accounts for the specific P_0 deficit observed in senescent diaphragms compared to adults. Further, since in this *in vitro* preparation, a given unit area of myofibrillar protein produced the same amount of force in both adult and senescent diaphragms, it is inferred that any possible age-related alterations in excitation-contraction coupling and/or the intrinsic properties of the contractile proteins did not contribute to the specific P_0 deficit.

As noted above, a reduction in the relative contribution of myofibrillar protein to the total CSA could occur by increasing the quantity of some non-contractile material.

Therefore, to determine which non-contractile component(s) of muscle were responsible for the age-related reduction in diaphragm myofibrillar protein concentration, the concentrations of connective tissue and water were determined in the costal diaphragm. This allows the assessment of the role of connective tissue and water on the specific P_0 production both separately and together. This analysis reveals that elimination of the contribution of connective tissue to the strip CSA only slightly reduces the senescent specific force deficit; whereas, elimination of the contribution of water to the strip CSA reduces the senescent specific P_0 deficit by 61% (from -16.4% to -6.4%). Finally, elimination of both connective tissue and water from the strip CSA results in no differences between adult and senescent specific forces (figure 5). These data confirm that the senescent specific P_0 deficit is a function of reduced myofibrillar protein concentration due to increases in water and connective tissue concentration with water being the primary factor.

Correlational analyses reveal significant relationships between specific P_0 and relative dry mass of the diaphragms and connective tissue concentration (figure 6). The relatively low coefficients of determination can be explained by the variation in specific P_0 and dry mass/connective tissue concentration within the separate age groups. In other words, the natural variation in specific P_0 within each age group cannot be explained or predicted by variations in dry mass and/or connective tissue concentration, even though the specific P_0 variation between age groups can be explained by these factors.

Diaphragmatic Skinned Single Fiber Measurements

The data presented in tables 7 and 8 represent the first comparison of contractile characteristics of single diaphragm fibers from mature adult and senescent animals. A recent study has compared the contractile characteristics of skinned single fibers isolated from locomotor muscle of adult (6-9 months old) and senescent (27 months old) rats (81).

Similar to the present findings in the diaphragm, these investigators reported no age-related changes in the specific F_0 of fast- and slow-twitch fibers. The lack of age-related change in the specific F_0 lends further support to the conclusion that the intrinsic force generating capacity of the sarcomeres of aging diaphragm muscle is not altered. This conclusion agrees with data examining force production in locomotor muscles (82).

The mean fiber CSA, single fiber maximal calcium-activated tetanic force (F_0), and specific F_0 ($\text{mN} \cdot \text{mm}^{-2}$) in the present study are in agreement with published values presented for type I (slow) fibers from adult rat diaphragm (83). However, the mean specific F_0 for type II fibers in the present study is lower (~25%) than the mean specific F_0 for fast fibers presented by Eddinger and Moss (83). Further, the mean type I and type II fiber specific F_0 presented in the present study are 30-40% lower than specific F_0 values reported for skinned single fibers from adult locomotor muscles (84, 85). One possible reason for this discrepancy in diaphragmatic type II fiber specific F_0 is that Eddinger and Moss (83) classified fibers based on single fiber V_{max} and ATPase histochemistry. Therefore, the fibers in this study labeled as "fast" may have been predominantly type IIb fibers. Examination of individual single fiber F_0 (table 8) from the present study indicates that the specific F_0 for the type IIb fibers tend to be higher than the mean specific F_0 reported for all type II fibers. Although the sample size was too small for statistical comparison of each type II MHC phenotype separately, the proportion of each phenotype sampled is similar for both adult and senescent groups; therefore, combining all type II fibers for group comparison should yield a valid conclusion. A possible reason for the lower specific F_0 values in the present study, as compared to locomotor muscle fibers, involves the method employed to determine the CSA of the single fibers. In the present study, the diameter of each single fiber at L_0 was measured with the fiber submerged at a constant depth in relaxing solution. Subsequent comparison of fiber diameters obtained using this method with diameters of the same fibers measured in air reveals a constant ~20% increase in the submerged fiber diameter compared to the fiber in air. Theoretical

calculations indicate that inflation of a fiber diameter by 20% would result in a consistent 31% reduction in the calculated specific F_0 . This accounts for the discrepancy between the present data and the locomotor muscle fiber specific F_0 cited above (84, 85), since these investigators did, in fact, measure fiber diameters in air.

Age-Related Changes in Shortening Velocity of the Diaphragm

The age-related increase in diaphragmatic V_{\max} observed in the present data is a unique finding and contradicts previous reports of unaltered (14) or decreased (12) V_{\max} in locomotor skeletal muscle of senescent rodents. Despite the age-related reduction in maximal diaphragmatic force generation, comparison of the *in vitro* diaphragmatic power curves for adult and senescent animals (figure 2) revealed no obvious age-related differences in diaphragmatic power over the range of isotonic specific forces surrounding maximal power production. Further, maximal power did not differ between groups (table 2). This suggests that the senescent diaphragm may have effectively compensated for its reduced force generating capacity by increasing its velocity of shortening. It is unknown whether this alteration is a direct adaptation to the decreased force generating capacity of the diaphragm or if it is the result of some other change in the aging diaphragm.

Since V_{\max} is thought to be primarily determined by the rate of ATP hydrolysis by the myofibrillar ATPase enzyme (4), it was postulated that the underlying mechanism for the aging increase in V_{\max} was an increase in the maximal myofibrillar ATPase activity in the diaphragm. Also, that the relative proportions of the fast (type II) MHC isoforms would be increased in the senescent diaphragms. The second postulate was supported by the data showing a large increase in the relative proportion of type IIb MHC in the senescent diaphragms as compared to the adults. Interestingly, the proportion of type I MHC was also increased in the senescent diaphragms (table 9). This paradoxical increase in the MHC isoforms possessing both the fastest (type IIb) and the slowest (type I) ATPase activities

may explain why myofibrillar ATPase activity did not differ statistically between the age groups. It appears that the aging diaphragm may be subject to two separate and opposing mechanisms. One mechanism, common to all aging skeletal muscle, causes a shift in MHC expression from fast-to-slow (29, 30). A second mechanism, unique to the diaphragm, causes a shift in MHC expression from slow-to-fast (36). The first mechanism may be the result of an age related hypothyroidism (49), but the second mechanism remains a mystery. One possibility is that there is a change in the neural output to the diaphragm as the animal ages which differs from the aging changes in neural output to locomotor muscles. Support for this notion can be found in a study of the neuromuscular junctions of young and old mice (86). These investigators reported that mean resting membrane potentials and miniature end plate potential (m.e.p.p.) amplitudes were higher in the old diaphragms as compared to the young. Further, they found that the m.e.p.p. frequency did not differ between young and old diaphragms whereas m.e.p.p. frequency was reduced in the old locomotor muscles examined. The significance of these findings are unclear but provide a direction for future research.

There are three primary factors that determine the velocity of shortening of skeletal muscle when expressed in units of muscle lengths per second: 1) length of the sarcomeres, 2) cross-bridge cycling rate, and 3) cross-bridge shortening distance per molecule of ATP hydrolyzed. Comparative physiologists have observed that, across species, speed of shortening is inversely correlated with sarcomere length (87, 88). This is presumably due to an increased number of shortening units in series. Nevertheless, no evidence exists to suggest that sarcomere length changes with aging. The theory proposed by A. F. Huxley (89) describing thick and thin filament interactions remains the most widely accepted model of muscular contraction (shortening and force generation). In this model, sarcomere shortening is the result of three steps: the attachment of the cross-bridge to actin, the "working stroke" of the cross-bridge, and the detachment of the cross-bridge. Shortening velocity is limited by the rate constant for dissociation of the myosin head from the actin

active site which, in turn, is closely associated with the hydrolysis of ATP. As noted previously, myofibrillar ATPase activity is closely related to V_{\max} in skeletal muscle; however, recent reports suggest that the cross-bridge shortening stroke may be subject to alterations independent of ATPase activity. For example, Maruyama et al. (90) found that V_{\max} is reduced in isolated single fibers after incubation of the fibers in ethylene glycol. Based on this data and the relationship between shortening velocity and ATP concentration in the ethylene glycol treated fibers, these authors concluded that this treatment reduced both actomyosin ATPase activity and the shortening distance per mole of hydrolyzed ATP. Hofmann et al. (91) reported that extraction of C-protein from isolated rabbit muscle skinned fibers resulted in an increase in V_{\max} at submaximal levels of calcium activation. Since C-protein is known to be involved in the structure of the thick filament (91), its removal may alter the mechanics of the cross-bridge stroke. Finally, Lowey et al. (92) studied the *in vitro* movement of actin filaments across stationary S1 myosin fragments (which contain the ATPase enzyme and the light chain binding regions) and found that complete extraction of the myosin light chains resulted in a dramatic reduction in the velocity of actin movement without altering the ATPase activity of the myosin fragments. These data indicate that under certain conditions, changes in muscle V_{\max} may be attributable to factors other than changes in myofibrillar ATPase activity.

In the present study, correlational analyses of the relationships between V_{\max} and both myofibrillar ATPase activity and percentage of type IIb MHC (table 10) suggest that other mechanism(s), in addition to the increase in type IIb MHC proportion, must be involved in mediating the dramatic increase in V_{\max} in the aging diaphragm. It is possible that some unknown age-related change in the rat diaphragm causes an increase in the sarcomere shortening distance per mole of ATP hydrolyzed. This remains an interesting area for future research.

Summary and Conclusions

It has been noted that the maximal *in vitro* specific P_0 of a muscle is determined by the following factors: the maximal force generated by the individual force generating units (i.e. cross-bridges), the proportion of myofibrils per unit of muscle CSA, and the degree of sarcomere activation via excitation-contraction coupling. The present study was designed to systematically examine these factors to determine the mechanism responsible for the age-related deficit in specific P_0 observed in the rat diaphragm. This was accomplished by examining the components of the diaphragm muscle (i.e. myofibrillar protein, water, and connective tissue) in adult (9 month old) and senescent (26 month old) male Fischer 344 rats, and normalizing diaphragmatic *in vitro* force production to strip myofibrillar protein CSA, connective tissue-free CSA, dry mass CSA, and dry, connective tissue-free CSA. Further, the maximal calcium-activated specific force (specific F_0) in diaphragmatic skinned single fibers was also assessed. Theoretically, if an age-related change in the force generating capacity of individual cross-bridges was primarily responsible for the aging specific P_0 deficit, then diaphragm strip P_0 normalized to myofibrillar protein CSA and single fiber specific F_0 would also demonstrate an age-related deficit. If aging changes in the excitation-contraction coupling mechanism were primarily responsible for the aging specific P_0 deficit, then diaphragm strip P_0 normalized to myofibrillar protein CSA would exhibit an age-related deficit but single fiber specific F_0 would not. Finally, if an age-related alteration in diaphragmatic myofibrillar protein concentration was primarily responsible for the aging specific P_0 deficit, then neither diaphragm strip P_0 normalized to myofibrillar protein CSA nor single fiber specific F_0 would exhibit the age-related force deficit.

The results of this study show that normalization of diaphragmatic *in vitro* force to myofibrillar protein CSA eliminates the difference observed in specific P_0 between adult and senescent diaphragms. Also, that specific F_0 of diaphragmatic skinned single fibers

does not differ between adult and senescent animals. Therefore, an age-related reduction in the proportion of myofibrils per unit area of diaphragm muscle is identified as the primary factor mediating the senescent specific P_0 deficit. Further, the data indicate that the aging-induced reduction in relative myofibrillar protein CSA primarily results from an age-related increase in diaphragmatic water content, with an increase in connective tissue concentration and possibly a decrease in total myofibrillar protein content also contributing. The age-related increase in diaphragmatic connective tissue concentration occurs in the extracellular compartment as can be seen in the histochemical connective tissue data presented in the present study (figure 3). However, the location (i.e. intracellular vs. extracellular) as well as the underlying mechanism(s) of the aging-induced increase in diaphragmatic water content remains unknown. This provides an intriguing avenue for future research in the area of aging muscle.

Another finding of this study is that diaphragmatic V_{max} is increased by 17.5% in the senescent animals as compared to the adults. This is apparently due in part to an increase in the proportion of type IIb MHC in the aging diaphragm. This could occur by an upregulation of the type IIb MHC gene and/or a decrease in the degradation rate of this protein relative to the other myosin isoforms. The age-related change in V_{max} may be a neurally mediated adaptation to the decreasing force generating capacity of the diaphragm as the animal ages. This is very speculative and provides an interesting area for future research.

REFERENCES

1. Black, L. F. and R. Hyatt. Maximal respiratory pressures: normal values and relationships to age and sex. Am. Rev. Respir. Dis. 99: 696-702, 1969.
2. Murray, J. F. The Normal Lung. Second edition. Philadelphia: W. B. Saunders Company. 1986; pp. 339-360.
3. Zhang, Y. and S. G. Kelsen. Effects of aging on diaphragm contractile function in golden hamsters. Am. Rev. Respir. Dis. 142: 1396-1401, 1990.
4. Close, R. Dynamic properties of mammalian skeletal muscle. Physiol. Rev. 52: 129-197, 1972.
5. Taylor, J. and S. Kandarian. Advantage of normalizing force production to myofibrillar protein in skeletal muscle cross-sectional area. J. Appl. Physiol. 76(2): 974-978, 1994.
6. Klitgaard, H., M. Mantoni, S. Schiaffino, S. Ausoni, L. Gorza, C. Laurent-Winter, P. Schohr, and B. Saltin. Function, morphology and protein expression of ageing skeletal muscle: a cross-sectional study of elderly men with different training backgrounds. Acta Physiol. Scand. 140: 41-54, 1990.
7. Daw, C., J. Starnes, and T. White. Muscle atrophy and hypoplasia with aging: impact of training and food restriction. J. Appl. Physiol. 64(6): 2428-2432, 1988.
8. Lexell, J., C. Taylor, and M. Sjostrom. What is the cause of the ageing atrophy? Total number, size and proportion of different fiber types studied in whole vastus lateralis muscle from 15- to 83-year-old men. J. Neurol. Sci. 84: 275-294, 1988.
9. Eddinger, T., R. Cassens, and R. Moss. Mechanical and histochemical characterization of skeletal muscles from senescent rats. Am. J. Physiol. 251(Cell Physiol. 20): C421-C430, 1986.
10. Klitgaard, H., A. Brunet, B. Malton, C. Lamaziere, C. Lesty, and H. Monod. Morphological and biochemical changes in old rat muscles: effect of increased use. J. Appl. Physiol. 67(4): 1409-1417, 1989.
11. Larsson, L., G. Grimby, and J. Karlsson. Muscle strength and speed of movement in relation to age and muscle morphology. J. Appl. Physiol. 46(3): 451-456, 1979.
12. Fitts, R., J. Troup, F. Witzmann, and J. O. Holloszy. The effect of ageing and exercise on skeletal muscle function. Mech. Ageing Dev. 27: 161-172, 1984.
13. Klitgaard, H., R. Marc, A. Brunet, H. Vandewalle, and H. Monod. Contractile properties of old rat muscles: effect of increased use. J. Appl. Physiol. 67(4): 1401-1408, 1989.

14. Brooks, S. and J. Faulkner. Contractile properties of skeletal muscles from young, adult and aged mice. J. Physiol. 404: 71-82, 1988.
15. Aniansson, A., M. Hedberg, G.-B. Henning, and G. Grimby. Muscle morphology, enzymatic activity, and muscle strength in elderly men: a followup study. Muscle Nerve 9: 585-591, 1986.
16. Larsson, L., B. Sjodin, and J. Karlsson. Histochemical and biochemical changes in human skeletal muscle with age in sedentary males, age 22-65 years. Acta Physiol. Scand. 103: 31-39, 1978.
17. Grimby, G., B. Danneskiold-Samsøe, K. Hvid, and B. Saltin. Morphology and enzymatic capacity in arm and leg muscles in 78-81 year old men and women. Acta Physiol. Scand. 115: 125-134, 1982.
18. Coggan, A., R. Spina, D. King, M. Rogers, M. Brown, P. Nemeth, and J. O. Holloszy. Histochemical and enzymatic comparison of the gastrocnemius muscle of young and elderly men and women. J. Gerontol. Biol. Sci. 46B: 71-76, 1992.
19. Meredith, C., W. Frontera, E. Fisher, V. Hughes, J. Herland, J. Edwards, and W. Evans. Peripheral effects of endurance training in young and old subjects. J. Appl. Physiol. 66: 2844-2849, 1989.
20. Kovanen, V. and H. Suominen. Effects of age and life-time physical training on fiber composition of slow and fast skeletal muscle in rats. Pflugers Arch. 408: 543-551, 1987.
21. Sanchez, J., C. Bastien, and H. Monod. Enzymatic adaptations to treadmill training in skeletal muscle of young and old rats. Eur. J. Appl. Physiol. 52: 69-74, 1983.
22. Cartee, G. and R. Farrar. Muscle respiratory capacity and VO_2 max in identically trained young and old rats. J. Appl. Physiol. 63: 257-261, 1987.
23. Brooke, M. and K. Kaiser. Three "myosin adenosine triphosphase" systems: the nature of their pH and sulphhydryl dependence. J. Histochem. Cytochem. 18: 670-672, 1970.
24. Eddinger, T., R. Moss, R. Cassens. Fiber number and type composition in extensor digitorum longus, soleus, and diaphragm muscles with aging in Fischer 344 rats. J. Histochem. Cytochem. 33: 1033-1041, 1985.
25. Larsson, L. and L. Edstrom. Effects of age on enzyme-histochemical fiber spectra and contractile properties of fast- and slow-twitch skeletal muscles in the rat. J. Neurol. Sci. 76: 69-89, 1986.
26. Staron, R., and D. Pette. The multiplicity of combinations of myosin light chains and heavy chains in histochemically typed single fibers: rabbit tibialis anterior muscle. Biochem. J. 243: 695-699, 1987.
27. Klitgaard, H., M. Zhou, S. Schiaffino, R. Betto, G. Salvati, and B. Saltin. Ageing alters the myosin heavy chain composition of single fibers from human skeletal muscle. Acta Physiol. Scand. 140: 55-62, 1990.

28. Sullivan, V.K. The effects of endurance exercise on myosin heavy chain composition in skeletal muscle of senescent rats. Master's thesis, University of Florida, 1993.
29. Sugiura, T., H. Matoba, H. Miyata, Y. Kawai, and N. Murakami. Myosin heavy chain transition in ageing fast and slow muscles of the rat. Acta Physiol. Scand. 144: 419-423, 1992.
30. Larsson, L., D. Biral, M. Campione, and S. Schiaffino. An age-related type IIb to IIx myosin heavy chain switching in rat skeletal muscle. Acta Physiol. Scand. 147: 227-234, 1993.
31. Nakano, M., H. Baba, H. Tauchi, and T. Sato. Age-related change in activation by Tris (hydroxymethyl) aminomethane on myosin-ATPase activity of human minor pectoral muscles. Mech. Ageing Dev. 31: 187-195, 1985.
32. Taylor, A., E. Noble, D. Cunningham, D. Paterson, and P. Rechnitzer. Ageing, skeletal muscle contractile properties and enzymatic activities with exercise. In: Sato, Y., J. Poortmans, I. Hashimoto, and Y. Oshida, eds. Integration of Medical and Sports Sciences, Med. Sport Sci. Basel: Karger, 37:109-125, 1992.
33. Srivastava, S. and M. Kanungo. Aging modulates some properties of skeletal myosin ATPase of the rat. Biochem. Med. 28: 266-272, 1982.
34. Florini, J. R. and D. Ewton. Skeletal muscle fiber types and myosin ATPase activity do not change with age of growth hormone administration. J. Gerontol. 44(5): B110-B117, 1989.
35. Gosselin, L. E., M. Betlach, A. Vailas, M. Greaser, and P. Thomas. Myosin heavy chain composition in the rat diaphragm: effect of age and exercise training. J. Appl. Physiol. 73(4): 1282-1286, 1992.
36. Gosselin, L., B.D. Johnson, and G. Sieck. Age-related changes in diaphragm muscle contractile properties and myosin heavy chain isoforms. Am. Rev. Resp. Dis. (In press).
37. Powers, S. K., J. Lawler, D. Criswell, F.-K. Lieu, and S. Dodd. Alterations in diaphragmatic oxidative and oxidative enzymes in the senescent Fischer 344 rat. J. Appl. Physiol. 72(6): 2317-2321, 1992.
38. Powers, S. K., D. Criswell, F.-K. Lieu, S. Dodd, and H. Silverman. Diaphragmatic fiber type specific adaptation to endurance exercise. Respiration Physiol. 89: 195-207, 1992.
39. Powers, S. K., D. Criswell, F.-K. Lieu, S. Dodd, and H. Silverman. Exercise-induced cellular alterations in the diaphragm. Am. J. Physiol. 263(Regulatory Integrative Comp. Physiol. 32): R1093-R1098, 1992.
40. Pette, D. and G. Vrbova. Neural control of phenotypic expression in mammalian muscle fibers. Muscle Nerve 8: 676-689, 1985.
41. Larsson, L. Aging in mammalian skeletal muscle. In: Mortimer, J., F. Pirozzolo, and G. Maletta (eds.) Advances in neurogerontology vol. 3, The Aging Motor System New York: Praeger, 1982, p. 258.

42. Takagi, A. and M. Endo. Guinea pig soleus and extensor digitorum longus: a study on single fibers. Exp. Neurol. 55: 95-101, 1977.
43. Nwoye, Luke, W. F. H. M. Mommaerts, D. R. Simpson, K. Seraydarian, and M. Marusich. Evidence for a direct action of thyroid hormone in specifying muscle properties. Am. J. Physiol. 242(Regulatory Integrative Comp. Physiol. 11): R401-R408, 1982.
44. Izumo, Seigo, Bernardo Nadal-Ginard, and Vijak Mahdavi. All members of the MHC multigene family respond to thyroid hormone in a highly tissue-specific manner. Science 231(February 7): 597-600, 1986.
45. Caiozzo, V. J., R. Herrick, and K. Baldwin. Influence of hyperthyroidism on maximal shortening velocity and myosin isoform distribution in skeletal muscles. Am. J. Physiol. 261(Cell Physiol. 30): C285-C295, 1991.
46. Caiozzo, V. J., R. Herrick, and K. Baldwin. Response of slow and fast muscle to hypothyroidism: maximal shortening velocity and myosin isoforms. Am. J. Physiol. 263(Cell Physiol. 32): C86-C94, 1992.
47. Montgomery, A. The time course of thyroid-hormone-induced changes in the isotonic and isometric properties of rat soleus muscle. Pflugers Arch. 421: 350-356, 1992.
48. Everts, M., C. van Hardevelde, H. Ter Keurs, and A. Kassenaar. Force development and metabolism in skeletal muscle of euthyroid and hypothyroid rats. Acta Endocrinol. 97: 221-225, 1981.
49. Segal, J., B. Troen, and S. Ingbar. Influence of age and sex on the concentrations of thyroid hormone in serum in the rat. J. Endocrinol. 93: 177-181, 1982.
50. Carter, W., W. Kelly, F. Faas, M. Lynch, and C. Perry. Effect of graded doses of triiodothyronine on ventricular myosin ATPase activity and isomyosin profile in young and old rats. Biochem. J. 247: 329-334, 1987.
51. Rotwein, P. S. Insulin-like growth factors in muscle growth and differentiation. In: Sizonenko, P. and M. Aubert (eds.) Developmental Endocrinology New York: Raven Press, 1990, pp. 155-163.
52. Vandeburgh, H., P. Karlisch, J. Shansky, and R. Feldstein. Insulin and IGF-I induce pronounced hypertrophy of skeletal myofibers in tissue culture. Am. J. Physiol. 260: C475-C484, 1991.
53. Sonntag, W. E., J. Lenham, and R. Ingram. Effects of aging and dietary restriction on tissue protein synthesis: relationship to plasma insulin-like growth factor-1. J. Gerontol. 47(5): B159-B163, 1992.
54. Kandarian, S. and T. White. Force deficit during the onset of hypertrophy. J. Appl. Physiol. 67: 2600-2607, 1989.
55. Kovanen, V. Effects of aging and physical training on rat skeletal muscle. Acta Physiol. Scand. 135(Suppl. 577): 1-56, 1989.
56. Alnaqeeb, M. A., N. Zaid, and G. Goldspink. Connective tissue changes and physical properties of developing and ageing skeletal muscle. J. Anat. 139: 677-689, 1984.

57. Boreham, C. A. G., P. Watt, P. Williams, B. Merry, G. Goldspink, and D. Goldspink. Effects of ageing and chronic dietary restriction on the morphology of fast and slow muscles of the rat. J. Anat. 157: 111-125, 1988.
58. Kandarian, S., R. Boushel, and L. Schulte. Elevated interstitial fluid volume in rat soleus muscles by hindlimb unweighting. J. Appl. Physiol. 71(3): 910-914, 1991.
59. Jaiswal, Y. K., and M. S. Kanungo. Expression of actin and myosin heavy chain genes in skeletal, cardiac and uterine muscles of young and old rats. Biochem. Biophys. Res. Comm. 168(1): 71-77, 1990.
60. Gafni, A. and K. Yuh. A comparative study of Ca^{+2} - Mg^{+2} dependent ATPase from skeletal muscles of young, adult and old rats. Mech. Ageing Dev. 49: 105-117, 1989.
61. Larsson, L. and G. Salvati. Effects of age on calcium transport activity of sarcoplasmic reticulum in fast- and slow-twitch rat muscle fibers. J. Physiol. 419: 253-264, 1989.
62. Hazzard, D. G., R. Bronson, G. McClearn, and R. Strong. Guest Editorial: selection of an appropriate animal model to study aging processes with special emphasis on the use of rat strains. J. Gerontol. 47(3): B63-B64, 1992.
63. Metzger, J. and R. Fitts. Contractile and biochemical properties of diaphragm: effects of exercise and fatigue. J. Appl. Physiol. 60: 1752-1758, 1986.
64. Woledge, R., N. Curtin, and E. Homsher. Energetic Aspects of Muscle Contraction. Academic Press. New York. 1985.
65. Solaro, R. J., D. Pang, and F. N. Briggs. The purification of cardiac myofibrils with Triton X-100. Biochim. Biophys. Acta 245: 259-262, 1971.
66. Watters, C. A one-step biuret assay for protein in the presence of detergent. Anal. Biochem. 88: 695-698, 1978.
67. Segal, S., T. White, and J. Faulkner. Architecture, composition and contractile properties of rat soleus and muscle grafts. Am. J. Physiol. 250: C474-C479, 1986.
68. Talmadge, R.J. and R. Roy. Electrophoretic separation of rat skeletal muscle myosin heavy-chain isoforms. J. Appl. Physiol. 75(5): 2337-2340, 1993.
69. Kandarian, S. and T. White. Force deficit persists during long-term muscle hypertrophy. J. Appl. Physiol. 69: 861-867, 1990.
70. Blanco, C., G. Sieck, and V. Edgerton. Quantitative histochemical determination of succinate dehydrogenase activity in skeletal muscle fibers. Histochem. J. 20: 230-243, 1988.
71. Powers, S. K., F.-K. Lieu, D. Criswell, and S. Dodd. Biochemical verification of quantitative histochemical analysis of succinate dehydrogenase activity in skeletal muscle fibers. Histochem. J. 25: 491-496, 1993.
72. Constantine, V.S. A combined tissue stain for the selective staining of collagen, elastin fibers and acidic carbohydrates. J. Invest. Dermatol. 52: 353-356, 1969.

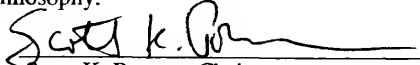
73. Gollnick, P.D., B. Timson, R. Moore, and M. Riedy. Muscular enlargement and number of fibers in skeletal muscles of rats. J. Appl. Physiol. 50: 936-943, 1981.
74. Moss, R., G. Giulian, and M. Greaser. Effects of EDTA treatment upon the protein subunit composition and mechanical properties of mammalian single skeletal muscle fibers. J. Cell Biol. 96: 970-978, 1983.
75. Fabiato, A. Computer programs for calculating total and specific free or free from specified total ionic concentrations in aqueous solutions containing multiple metals and ligands. Methods in Enzymol. 157: 378-417, 1988.
76. Diffie, G., V. Caiozzo, R. Herrick, and K. Baldwin. Contractile and biochemical properties of rat soleus and plantaris after hindlimb suspension. Am. J. Physiol. 260(Cell Physiol. 29): C528-C534, 1991.
77. Finol, H., D. Lewis, and R. Owens. The effects of denervation on contractile properties of rat skeletal muscle. J. Physiol. 319: 81-92, 1981.
78. Zimmerman, S., R. McCormick, R. Vadlamudi, and P. Thomas. Age and training alter collagen characteristics in fast- and slow-twitch rat limb muscle. J. Appl. Physiol. 75(4): 1670-1674, 1993.
79. Gosselin, L., D. Martinez, A. Vailas, and G. Sieck. Passive length-force properties of the senescent diaphragm: relationship to collagen characteristics. J. Appl. Physiol. 76(6): 2680-2685, 1994.
80. Aukland, K., and G. Nicolaysen. Interstitial fluid volume: local regulatory mechanisms. Physiological Rev. 61(3): 556-643, 1981.
81. Lynch, G., B. Rodgers, and D. Williams. The effects of age and low-intensity endurance exercise on the contractile properties of single skinned fast- and slow-twitch skeletal muscle fibers. Growth Dev. Aging 57: 147-161, 1993.
82. Ansved, T., and L. Larsson. Effects of ageing on enzyme-histochemical, morphometrical and contractile properties of the soleus muscle in the rat. J. Neurological Sci. 93: 105-124, 1989.
83. Eddinger, T., and R. Moss. Mechanical properties of skinned single fibers of identified types from rat diaphragm. Am. J. Physiol. 253(Cell Physiol. 22): C210-C218, 1987.
84. Kandarian, S., and J. Williams. Contractile properties of skinned fibers from hypertrophied skeletal muscle. Med. Sci. Sports Exerc. 25(9): 999-1004, 1993.
85. Williams, J., C. Ward, and G. Klug. Fatigue-induced alterations in Ca^{2+} and caffeine sensitivities of skinned muscle fibers. J. Appl. Physiol. 75(2): 586-593, 1993.
86. Banker, B., S. Kelly, and N. Robbins. Neuromuscular transmission and correlative morphology in young and old mice. J. Physiol. 339: 355-375, 1983.
87. Huxley, A.F., and R. Simmons. Mechanical transients and the origin of muscular force. Cold Spring Harbor Symposia on Quantitative Biol. 67: 669-680, 1972.

88. Atwood, H., G. Hoyle, and T. Smyth. Mechanical and electrical responses of single innervated crab muscle fibers. J. Physiol. 180: 449, 1965.
89. Huxley, A.F. Muscle structure and theories of contraction. Prog. Biophys. Biophys. Chem. 7: 255-318, 1957.
90. Maruyama, T., K. Kometani, and K. Yamada. Modification of the contractile properties of rabbit skeletal muscle by ethylene glycol. J. Biochem. (Tokyo) 105: 1009-1013, 1989.
91. Hofmann, P., M. Greaser, and R. Moss. C-protein limits shortening velocity of rabbit skeletal muscle fibers at low levels of Ca^{2+} activation. J. Physiol. 439: 701-715, 1991.
92. Lowey, S., G. Waller, and K. Trybus. Skeletal muscle myosin light chains are essential for physiological speeds of shortening. Nature 365: 454-456, 1993.

BIOGRAPHICAL SKETCH

David S. Criswell graduated from the University of Mississippi in 1988 with a Bachelor of Science degree in biology. An interest in the scientific basis of sport and exercise led him to pursue graduate studies in the field of exercise physiology. In 1990 he earned a Master of Science in Exercise and Sport Sciences at the University of Florida. David continued his graduate work at the University of Florida, under the direction of Dr. Scott K. Powers, focusing on the adaptive responses of skeletal muscle to various stimuli including exercise training, pharmacological treatments, and aging. Upon receiving a Ph.D. in Health and Human Performance, David has accepted a postdoctoral training fellowship at the University of Texas Medical School in Houston, under the direction of Dr. Frank Booth.

I certify that I have read this study and that in my opinion it conforms to acceptable standards of scholarly presentation and is fully adequate, in scope and quality, as a dissertation for the degree of Doctor of Philosophy.



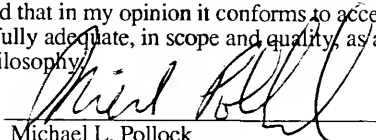
Scott K. Powers, Chair
Professor of Exercise and Sport Sciences

I certify that I have read this study and that in my opinion it conforms to acceptable standards of scholarly presentation and is fully adequate, in scope and quality, as a dissertation for the degree of Doctor of Philosophy.



Stephen L. Dodd
Associate Professor of Exercise and Sport Sciences

I certify that I have read this study and that in my opinion it conforms to acceptable standards of scholarly presentation and is fully adequate, in scope and quality, as a dissertation for the degree of Doctor of Philosophy.



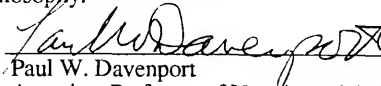
Michael L. Pollock
Professor of Exercise and Sport Sciences

I certify that I have read this study and that in my opinion it conforms to acceptable standards of scholarly presentation and is fully adequate, in scope and quality, as a dissertation for the degree of Doctor of Philosophy.



A. Daniel Martin
Associate Professor of Physical Therapy

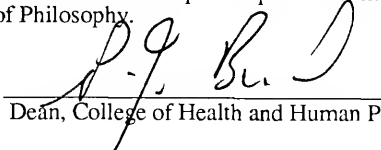
I certify that I have read this study and that in my opinion it conforms to acceptable standards of scholarly presentation and is fully adequate, in scope and quality, as a dissertation for the degree of Doctor of Philosophy.



Paul W. Davenport
Associate Professor of Veterinary Medicine

This dissertation was submitted to the Graduate Faculty of the College of Health and Human Performance and to the Graduate School and was accepted as partial fulfillment of the requirements for the degree of Doctor of Philosophy.

August 1994



Dean, College of Health and Human Performance

Dean, Graduate School

LD
1780
1994
.C933

